SLAC – PUB – 3573
February 1985
(T/E)

A SELECTIVE EXPERIMENTAL REVIEW OF THE STANDARD MODEL*

E. D. BLOOM

Stanford Linear Accelerator Center
Stanford University, Stanford, California 94305

Invited talk presented at the Aspen Winter Physics Conference
Aspen, Colorado, January 13-19, 1985

* Work supported by the Department of Energy, contract DE – AC03 – 76SF00515

Introduction and Summary

Before discussing experimental comparisons with the "Standard Model", (S-M) it is probably wise to define more completely what is commonly meant by this popular term. This model is a gauge theory of $SU(3)_f \times SU(2)_L \times U(1)$ with 18 parameters. The parameters are α_s, α_{qed}, θ_W, M_W ($M_Z \equiv M_W/\cos\theta_W$, and thus is not an independent parameter), M_{Higgs}; the lepton masses, M_e, M_μ, M_τ; the quark masses, M_d, M_s, M_b, and M_u, M_c, M_t; and finally, the quark mixing angles, $\theta_1, \theta_2, \theta_3$, and the CP violating phase δ. The latter four parameters appear in the quark mixing matrix as shown in Figure 1 for the Kobayashi-Maskawa[1] and Maiani[2] forms. Clearly, the present S-M covers an enormous range of physics topics, and I can only lightly cover a few such topics in this report.

The measurement of R_{hadron} is fundamental as a test of the running coupling constant α_s in QCD. I will discuss a selection of recent "precision" measurements of R_{hadron}, as well as some other techniques for measuring α_s. QCD also requires the self interaction of gluons. The search for the three gluon vertex may be practically realized in the clear identification of gluonic mesons. I will present a limited review of recent progress in the attempt to untangle such mesons from the plethora of $q\bar{q}$ states of the same quantum numbers which exist in the same mass range. The electroweak interactions provide some of the strongest evidence supporting the S-M that exists. Given the recent progress in this subfield, and particularly with the discovery of the W and Z bosons at CERN[3], many recent reviews[4] obviate the need for further discussion in this report. Finally, in attempting to validate a theory, one frequently searches for new phenomena which would clearly invalidate it. In that spirit I will examine recent searches for new particle states.

The Measurement of α_s

In this section I will discuss recent measurements of R_{hadron} which have systematic overall scale errors on the absolute value of R_{hadron} of $\pm 7\%$ or less. The most accurate measurements from the JADE[5] and MAC[6] collaborations are reported at the 2-3% level. The range in $\sqrt{s}$ of all the measurements is 5 to over 40 GeV, and thus the full combination of QCD and electroweak contributions to R_{hadron} must be considered.

In the quark-parton model the ratio $R_{hadron} = \sigma_{hadron}/\sigma_{\mu\mu}$ of the total hadronic cross section to the lowest order muon pair cross section is given by summing over the available quark flavors, n_f,

$$R_0(s) = 3\left(\sum_{q=1}^{n_f} Q_q^2 - v_e Re(g(s)) \sum_{q=1}^{n_f} Q_q v_q + \frac{1}{4}(v_e^2 + a_e^2)\,|g(s)|^2 \sum_{q=1}^{n_f}(v_q^2 + a_q^2)\right) \tag{1}$$

where Q_q are the quark charges, v_i and a_i are the neutral current vector and axial vector coupling constants of the electroweak theory[7], and

$$g(s) = \frac{1}{8\sin^2\theta_W \cos^2\theta_W}\left(\frac{s}{s - M_Z^2 + iM_Z\Gamma_Z}\right)$$

$$= \frac{G}{\sqrt{2}}\frac{1}{4\pi\alpha}\frac{sM_Z^2}{s - M_Z^2 + iM_Z\Gamma_Z} \quad . \tag{2}$$

It has been shown[8] that a rapidly converging perturbative expansion for R_{hadron} may be obtained from QCD ,

$$R_{hadron}(s) = R_o(s)\left(1 + \frac{\alpha_s}{\pi} + C\left(\frac{\alpha_s}{\pi}\right)^2\right) \quad . \tag{3}$$

Calculated in the modified minimal subtraction ($\overline{MS}$) scheme, one has $\overline{C} = 1.986 - 0.115 n_f$. Additional corrections are needed for finite quark mass effects near $q\bar{q}$ thresholds[8,9]. The coupling constant α_s is predicted in QCD to

run as a function of $\sqrt{s}$; the rate of the logarithmic decrease of α_s with increasing $\sqrt{s}$ is governed by $\Lambda_{\overline{MS}}$, the QCD scale parameter. Thus by determining α_s at one energy, the $\sqrt{s}$ dependence of R_{hadron} predicted in QCD can be checked, and at higher $\sqrt{s}$ the weak contribution to R_{hadron} can be measured in principle. The possibility of confronting theory with experiment depends on being able to measure R_{hadron} to within a few percent, given the present range of $\sqrt{s}$ available ($5 < \sqrt{s} < 45$ GeV). The difficulty of such measurements is partially illustrated in Figure 2 where a number of e^+e^- reactions are shown. Many of these reactions pose serious backgrounds to the process to be measured (in the cubby in the upper right of the figure). In addition, cosmic rays, beam gas interactions and other machine generated backgrounds can destroy the accuracy of an R_{hadron} measurement if not treated properly. Finally, the measurement of the integrated luminosity, typically using Bhabha scattering, is an important element in the accuracy of the measurement.

In order to best measure R_{hadron} certain detector features must be present, and an example of the generic R_{hadron} detector is shown in Figure 3. Illustrated in the figure are the requirements of large solid angle ($> 90\%$ of 4π), good hadron and electromagnetic calorimetry (over the entire solid angle), charged particle tracking (over most of the solid angle), and at least two independent measurements of the luminosity (large and small angle measurements, the latter with an independent apparatus), needed by a proper R_{hadron} detector.

Figure 4 illustrates the importance of a large solid angle. In this example from the MAC collaboration[6], distributions in two (of a number of) variables used to extract the hadronic events are shown as obtained from data and Monte Carlo. The agreement is excellent, giving confidence that the hadronic event extraction efficiency is well understood. A large acceptance of the detector allows for a large hadronic efficiency, and the ability to observe most of the event. Under such conditions, it is unlikely that the experimenters will be mislead by errant Monte Carlos, and even liberal error estimates on Monte Carlo param-

eters yield only a small contribution to the overall systematic error. Figure 5 illustrates the advantage of good calorimetry. This example from the Crystal Ball collaboration[10] demonstrates the ease of separating certain types of background. Using simple calorimetric variables obtained from only the energies and angles from each of the approximately 700 NaI(Tl) elements of the detector, an almost totally complete separation of cosmic ray events (real data) and hadronic events (Monte Carlo) is achieved. The need for independent measurements of the luminosity is shown in Figure 6 also using results from the Crystal Ball. In observing the differences in the two measurements, one can with confidence estimate the systematic errors (overall and point to point) coming from the luminosity; in the case of the Crystal Ball the systematic errors are $\pm 2.7\%$ overall, with an additional contribution from point to point[10].

Figure 7 shows selected R_{hadron} values from experiments which have systematic errors less than 7%. The statistical errors are added in quadrature with the quoted point to point systematic errors to yield the error bars shown in the figure. The rest of the (overall) systematic error of each experiment is given in the figure. Note that MAC reports a $\pm 2.3\%$ systematic error on their R_{hadron} value measured at $\sqrt{s} = 29$ GeV; this is the smallest error yet to be reported. Figure 8 repeats Figure 7 with the prediction of the simple parton model overlaid (electroweak effects are not included). The impression one obtained from Figure 8 is one of an increase in R_{hadron} at $b\bar{b}$ threshold, and a general excess over the simple parton model over the entire range of $\sqrt{s}$ shown. These qualitative impressions are in agreement with the expectations of QCD; however, as we shall see, quantitative comparisons are not particularly supportive of QCD.

Figure 9 shows results to higher values of $\sqrt{s}$ for the Mark-J[11] and TASSO[12] collaborations. Only beyond $\sqrt{s}$ of 40 GeV may one hope to see an effect from the purely weak contribution to R_{hadron}; however, the errors are still too large for a useful determination of the Weinberg angle. Also, the overall systematic uncertainty on R_{hadron} of about $\pm 5\%$ for these experiments precludes the pre-

cise determination of α_s needed to obtain the QCD baseline from which the electroweak contribution can be deduced at the high energies. Figure 10 demonstrates another difficulty; namely, at values of the Weinberg angle close to the presently accepted value of 0.23 the electroweak contribution to R_{hadron} (dominantly an interference term) has a zero. This makes the electroweak contribution even more difficult to detect in this energy range.

Of primary interest is how the value of R_{hadron} versus $\sqrt{s}$ quantitatively compares with the predictions of QCD. In order to attempt such a comparison for $\sqrt{s}$ below 40 GeV, a reliable determination of α_s at low energy is needed. Recently, the use of $\Upsilon(1S)$ decays has been considered to be reliable for such purposes. In particular the calculation of Mackenzie and Lepage[13] which determines α_s from a simple ratio of well measured $\Upsilon(1S)$ decays is particularly appealing:

$$\alpha_s^3(0.48M_\Upsilon) = \frac{\Gamma_{had}(\Upsilon)}{\Gamma_{\mu\mu}(\Upsilon)}\,\alpha_{QED}^2\,\frac{81\pi Q_b^2}{10(\pi^2-9)}\ , \tag{4}$$

α_s is defined to second order in the $\overline{MS}$ renormalization scheme by,

$$\alpha_s(\sqrt{s}) \equiv \frac{12\pi}{(33-2n_f)\ln(s/\Lambda^2_{\overline{MS}})}\left[1-\frac{462\ln\ln(s/\Lambda^2_{\overline{MS}})}{625\ln(s/\Lambda^2_{\overline{MS}})}\right]\ . \tag{5}$$

Application of equation (4) to the $\Upsilon(1S)$ data[14] yields the first value shown in Table 1 and $\Lambda_{\overline{MS}} = 118^{+16}_{-15}$ MeV. The other entries in Table 1 are obtained from R_{hadron} measurements as indicated in the table. That QCD is not well confirmed in its prediction of a decreasing α_s with increasing $\sqrt{s}$ is evident by examination of the table. Indeed, the MAC experiment alone shows almost a two standard deviation disagreement with the extrapolation of α_s from the $\Upsilon(1S)$ determination. However, it is clear that more data is needed, and with even smaller errors, to reliably check the QCD predictions.

Quarkonium and QCD

Another check of QCD of a qualitative nature is given by the comparison of the hadronic widths of the ${}^3P_J$ states of charmonium with those of bottomonium. Figure 11 shows the lowest order diagram in QCD perturbation theory describing the hadronic decay of the ${}^3P_0$ and ${}^3P_2$ states; two gluon emission is thought to mediate these decays. The diagram for the hadronic decay of the ${}^3P_1$ state is somewhat more involved[15]. Equations (6)-(8) give the lowest order QCD predictions for the decays[15],

$$\Gamma(1^3P_2 \rightarrow hadrons) = \frac{128}{5}\alpha_s^2 \frac{|\psi_1'(0)|^2}{M_\chi^4} \tag{6}$$

$$\Gamma(1^3P_1 \rightarrow hadrons) = \frac{128}{3\pi}\alpha_s^3 \frac{|\psi_1'(0)|^2}{M_\chi^4} \ln\left(\frac{4m_q^2}{4m_q^2 - M_\chi^2}\right) \tag{7}$$

$$\Gamma(1^3P_0 \rightarrow hadrons) = 96\alpha_s^2 \frac{|\psi_1'(0)|^2}{M_\chi^4} \ . \tag{8}$$

In the above equations the decay rates are all proportional to the derivative of the P-state wave function at the origin squared. Using a potential $V(r)$ which yields a 1S–2S mass spacing independent of quark flavor implies,

$$V(r) \sim \ln(r) \ , \tag{9}$$

and this in turn implies,

$$|\psi_1'(0)|^2 \sim M^{5/2} \ . \tag{10}$$

Taking all factors we find,

$$\frac{\Gamma_b(1^3P_2 \rightarrow hadrons)}{\Gamma_c(1^3P_2 \rightarrow hadrons)} \sim \left(\frac{\alpha_s(M_b)}{\alpha_s(M_c)}\right)^2 \frac{M_c^{3/2}}{M_b^{3/2}} \ . \tag{11}$$

Table 2 shows the numbers obtained from the experiments. The last four measurements in the table come from γ cascade decays of the $\Upsilon(2S)$ to the $\Upsilon(1S)$, and involve two assumptions. First, the lowest E_γ state observed is assumed to be the $^3P_2$ state, and the next lowest the $^3P_1$ state (the spins of these states are yet to be measured). Second, the partial width for the decay via a γ from the ^3P_J state to the $\Upsilon(1S)$ is taken from theory, *e.g.*, the CB uses Moxhay and Rosner[19]. (These are electric dipole transitions in the theory.) The theory combined with experiment then gives,

$$\Gamma_{had}(^3P_J) = \frac{Br^{exp}(\Upsilon' \to \gamma^3P_J) \times \Gamma_{E_1}(^3P_J \to \gamma\Upsilon)}{[Br(\Upsilon' \to \gamma^3P_J) \times Br(^3P_J \to \gamma\Upsilon)]_{exp}} \ . \tag{12}$$

One can then compare theory and experiment in ratio for the $c\bar{c}$ and $b\bar{b}$ systems. Theory predicts [equation (11)],

$$\frac{\Gamma^{b\bar{b}}_{had}(^3P_2)}{\Gamma^{c\bar{c}}_{had}(^3P_2)} \sim 0.11 \ , \tag{13}$$

while experiment gives 0.035 ± 0.028 for this ratio. Agreement is acceptable within the large errors and the assumptions made.

Gluonic Mesons – The Search for the Three Gluon Vertex of QCD

One of the most distinctive features of QCD, its non-Abelian character, has yet to be verified experimentally. Figure 12a shows this feature realized in lowest order. The implication of the existence of such a process in lowest order is physically realized in the prediction by QCD of the existence of an extensive spectrum of colorless, flavorless bound states of two or more gluons. It is expected that the lower mass states of these gluonic mesons are bound states of mostly two gluons, and their masses are predicted to lie in the range of 1 to 3 GeV/c^2. In this report I will briefly review the status of two states which have for some time

continued to hold the promise of containing a large gluonic meson component in their wave functions. These mesons are the $\iota(1440)$ and $\theta(1700)$, which have been primarily seen in the decay $J/\psi \to \gamma + X$ depicted in Figure 12b. (Though the ι may have first been seen in $p\bar{p}$ annihilation at rest[20].) Figure 13 briefly reviews the status of the ι. Part (a) of the figure indicates the level of information available as of 1982. The $K^+K^-\pi^0$ mass spectrum obtained from the decay of about 2 million J/ψ in the Crystal Ball [21] is shown with and without a $M_{K^+K^-}$ cut at the $\delta(980)$ mass. This data sample was used to first determine the J^P of the ι to be 0^-. The Mark II detector at SPEAR had previously seen this state in J/ψ decays, but was unable to measure its J^P; thus the state was erroneously identified as the $J^P = 1^+$ meson the E(1420)[16,23]. Recent results from the Mark III detector based on about 2.7 million J/ψ decays are shown in parts (b) and (c) of the figure; the $K_sK^\pm\pi^\mp$ and $K^+K^-\pi^0$ mass distributions are shown without a $K\overline{K}$ mass cut. This huge ι signal, and very little background, allows for a definitive J^P determination[24] of 0^-, thus confirming the result obtained by the Crystal Ball. All of the results are summarized in the table at the bottom of the figure. It should be noted that preliminary results from a recent BNL experiment AGS #771[25], have confirmed the 1^{++} $E(1420)$ in $p\pi$, and identified this state in $p\bar{p}$ annihilation in flight; however, the experimenters report that the situation is more complicated for $p\bar{p}$ at rest, the same reaction where Baillon *et al.*[20] first reported a 0^- state at the same mass.

Is the ι a gluonic meson? From the point of view of many theorists it has about the right mass and quantum numbers, and its big radiative decay rate from the J/ψ is also supportive of this interpretation. However, many other theorists disagree and classify the ι as a radially excited $q\bar{q}$ state. Seemingly, a way to settle the argument is to measure the radiative decays of the ι, since it is intuitive that a gluonic meson made from gluons having no charge should have a vanishingly small radiative decay, *i.e.*,

$$\frac{Br(\iota \to \gamma X)}{Br(\iota \to K\bar{K}\pi)} \ll 1\% \quad . \tag{14}$$

Figure 14 shows that this is likely not the case. The Crystal Ball[26] and Mark III[27] have measured the decay $J/\psi \to \gamma\gamma\rho^0$ and find a ratio of branching fractions (of what may be an ι related $\gamma\rho^0$ final state) to $\iota \to K\bar{K}\pi$ of the order of 1%. The experimental situation is not clear, however, since the enhancement seen in $\gamma\rho^0$ (see figure) is broader than the ι. Evidence that part of this structure is the ι is based on a preliminary spin analysis (see reference 24 for a review of the present situation). The theoretical explanation for the large radiative decay of the ι, involving a gluonic meson, is mixing of the pseudo-scalar mesons with a 0^- gluonic meson. The models in which the ι is mainly a $q\bar{q}$ state (radial excitation) easily accommodate a "large" radiative width; they would have difficulty explaining a "small" radiative width of the ι. The final status of the ι is yet to be settled.

Figures 15 and 16 briefly review the status of the $\theta(1700)$. Figure 15 shows the signals seen in $J/\psi \to \gamma X$, where in Figure 15a from the Crystal Ball[28] X is $\eta\eta$, and in 16b from the Mark II[22] X is K^+K^-. Clear signals are seen in both detectors; however, in the Crystal Ball result the statistics are limited, while for the Mark II there is a large background. Also shown in Figure 15c,d is the $\pi\pi$ mass spectrum in both detectors; no clear signal is seen. Both detectors, with varying confidence, determined the J^P of the θ to be 2^+. These results are reviewed in the table which makes up the top of Figure 16, along with recent results from the Mark III detector[29] and the DM2 detector operating at DCI[30]. Part (a) and (b) of the figure illustrate the data on which the Mark III tabular results are based. The data have clearly improved since 1982; good statistical information with little background is seen in the K^+K^- mass plot, and a signal is evident in the $\pi\pi$ mass spectrum at the θ mass. Using this data, the Mark III

was able to assign a J^P of 2^+ to the θ with high confidence, thus confirming the somewhat tentative assignments of the previous experiments.

Is the θ a gluonic meson? In my opinion it has always been the best candidate seen in J/ψ radiative decays due to its quantum numbers and mass[31]. The case would be particularly strong if the $\gamma\rho\rho$ final state first seen by the Mark II from the J/ψ with an enhancement at $M_{\rho\rho}$ about 1700 MeV[22] had J^P of 2^+. The Mark III collaboration has recently presented evidence that this enhancement, which also has a large radiative branching ratio from the J/ψ, was dominantly $J^P = 0^-$. However, the observation of a $\pi\pi$ final state of the θ has helped the gluonic meson interpretation. Thus, as in the case of the ι, the situation remains unresolved.

Of course the Υ system has hardly been explored when it comes to the question of gluonic mesons. The predicted production rates are quite small, and the existing samples of data are about a factor of 10 smaller than at the J/ψ; also, the detectors operating today are barely a match for this difficult region. However, as Figure 17 (and the previous 4 figures) illustrates, the progress at the J/ψ has been rapid and the surprises many; the Υ may have even more to offer.

New Particle Searches

The Search for Right Handed Currents

Beautiful precision experiments have been done on muon decay $\mu^+ \to \nu\bar{\nu}e^+$ to search for deviations from the S-M and right handed charged currents in particular. The experiments were performed at the TRIUMF meson factory by two somewhat overlapping groups, a Berkeley-SIN-TRIUMF group (B-S-T)[32], and a Berkeley-Northwestern-TRIUMF group (B-N-S)[33]. What I am presenting in this report has been presented in more detail in reference 34.

The muon differential decay rate, averaged over the e^+ polarization and to lowest non-vanishing order in M_e/M_μ, is given by,

$$\frac{d^2\Gamma}{x^2\,dx\,d\cos\Theta} \propto (3-2x) + (4\rho/3-1)(4x-3) + 12\frac{M_{e^+}}{M_{\mu^+}x}(1-x)\eta$$
$$- [(2x-1) + (4\delta/3-1)(4x-3)]\,\xi P_\mu \cos\theta\ , \quad (15)$$

where

$$x = \frac{E_{e^+}}{W}, \quad W = \frac{M_\mu^2 + M_e^2}{2M_\mu} \quad ,$$

and $\pi - \theta$ is the e^+ angle relative to the spin direction of the decaying μ^+, P_μ is the polarization of the μ^+, and ρ, η, ξ, and δ are the usual muon decay parameters[35] as calculated in the Standard Model.

The basic idea of the experiment I will discuss here is shown in Figure 18. The highly polarized muons are stopped in a magnetic field and allowed to decay. In one set of runs the field is 1.1 T parallel to the muon polarization, in another set of runs the field is 70 or 120 gauss perpendicular to the polarization direction. In the case shown in Figure 18, the field is parallel to the polarization direction and the spectrometer is observing backward e^+ near $x = 1$. This decay cannot occur due to angular momentum conservation unless right handed charged currents are contributing to the decay amplitude.

The experiments measured a number of parameters (sometimes in two ways) in order to obtain unprecedented limits on the mass of right handed W's, under the assumption that a right handed neutrino would be massless. Figure 19 shows some of the results of the experiments. The data presented in part (a) of the figure were used by the B-S-T collaboration to measure η. In the S-M, $\eta = 0$, the preliminary results of the measurement[32] yields,

$$\eta_{exp} = -0.087 \pm 0.097\ . \quad (16)$$

In the figure the S-M, with η fitted, is compared to the measurement. The small x end of the spectrum is particularly useful in this measurement, and the B-S-T

group working at TRIUMF has built a spectrometer optimized for the low energy end of the positron spectrum.

Figure 19b shows the data (and fit) used to extract a preliminary value for δ by the B-S-T collaboration. The S-M expects $\delta = 3/4$, and the fit, leaving ξP_μ free, but fixing ρ to the S-M value of 3/4, yields the "very preliminary" value,

$$\delta = 0.748 \pm 0.004 \pm 0.003 \; . \tag{17}$$

This is almost a factor of two improvement on the precision of the present world average.

Figure 20 shows the measurements of the positron endpoint spectrum (x near 1.0) by the B-N-S collaboration. Part (a) and (b) of the figure compare the spectra in x near the positron endpoint for $B_\perp$ equal 70 or 100 gauss, and $B_\parallel$ at 1.1 T, respectively. The effectively unpolarized spectrum in part (a) shows a characteristic sharp edge which is used to calibrate the spectrometer. That edge almost vanishes completely when, as shown in part (b), the strong longitudinal field holds the muon spin nearly anti-parallel to the positron direction. (There is a very small remnant edge left due to the finite acceptance of the spectrometer[34].) In order to minimize the effect of the finite acceptance of the spectrometer, data like those of Figure 20b (but divided into bins of $\cos\theta$), are plotted in Figure 20c, $\cos\theta$ versus $(\xi P_\mu \delta/\rho)\cos\theta$. The intercept at $\cos\theta = 1$ of the best fit line in the figure yields the limit[34] (which as we shall see is related to the limit on right handed currents),

$$\xi P_\mu \delta/\rho > 0.9959 \text{ (90\% C.L.)} \; . \tag{18}$$

When $B_\perp$ is applied as for the data of Figure 19a, the muon spin rotates and $\langle P_\mu \rangle = 0$. (V−A) induces a maximal muon spin rotation (μSR) asymmetry in the decay e^+ decay rate. When the muon lifetime is factored out of the time spectrum, the sinusoidal modulation in Figure 20d is obtained. The amplitude

of the pure (V−A) contribution would be reduced by a (V+A) admixture. This technique offers a measurement of $(\xi P_\mu \delta/\rho)$ which has rather different systematic biases than the previously described measurement[34]. Fitting the data of Figure 20d the B-N-S collaboration obtains[34],

$$\xi P_\mu \delta/\rho > 0.9948 \text{ (90\% C.L.)} . \tag{19}$$

For $U(1) \times SU(2)_L \times SU(2)_R$, the W mass eigenstates W_1 and W_2 need not be the same as the gauge bosons W_L and W_R, and so there can be a mixing matrix,

$$\begin{bmatrix} W_1 \\ W_2 \end{bmatrix} = \begin{bmatrix} \cos\varsigma & \sin\varsigma \\ -\sin\varsigma & \cos\varsigma \end{bmatrix} \begin{bmatrix} W_L \\ W_R \end{bmatrix} \tag{20}$$

If one defines a parameter α such that

$$\alpha \equiv M^2_{W_1}/M^2_{W_2} \quad , \tag{21}$$

ς and α are related to the experimentally measured quantities by,

$$\frac{\xi P_\mu \delta}{\rho} \simeq 1 - 2(2\alpha^2 + 2\alpha\varsigma + \varsigma^2) \tag{22}$$

with $M_{\nu_R} = 0$. One can then plot limits for ς versus alpha for the B-N-S experiment under the assumption that $M_{\nu_R} = 0$, and this is done in Figure 21. Also shown in in the figure is the only significant experimental constraint which does not depend on assumptions about the right handed neutrino mass from CDHS[36]. The limit on ς comes from the y distributions in νN and $\overline{\nu} N$ scattering where no right handed neutrino need be produced. For a review of limits with other assumptions on the right handed neutrino mass and from a number of experiments, see reference 34. Under somewhat restrictive assumptions, we thus find W_R mass limits of over 400 GeV from this B-N-S very low energy experiment. I find this a beautiful result.

The Search for Narrow States in the Radiative Decays of the J/ψ and Υ

First I will discuss results from the Mark II detector at SPEAR on a narrow state at a mass of 2.2 GeV/c^2 in J/ψ radiative decays. This is really a brief status report on this state, called the ξ, since it was first reported in conferences in the summer of 1983[37]. For a complete status report see the talk of R. Partridge in these proceedings[38].

Figure 22 shows the signal as seen in 1983 data and the sum of 1983 and 1984 data. In the 1983 sample of about 1.8 million J/ψ decays the signal is fitted as a 5 standard deviation (s.d.) effect; however, the sum of the 1982 and 1983 data, 2.6 millions J/ψ decays, shows a lower significance of 4.6 s.d. The best estimate of mass and width are[37],

$$m_\xi = (2.218 \pm 0.003 \pm 0.010)\,\mathrm{GeV/c^2}\ ,$$

$$\Gamma \leq 40\,\mathrm{MeV}\ (95\%\ \mathrm{C.L.})\ . \qquad (23)$$

The state is best seen in $J/\psi \to \gamma K^+K^-$, and the product branching ratio is

$$\mathrm{B}\,[J/\psi \to \gamma\xi(2.2)] \times \mathrm{B}(\xi \to K^+K^-) \ = \ (5.7 \pm 1.9 \pm 1.4) \times 10^{-5} \quad . \qquad (24)$$

The J^P of the state is not measured with the present data, but the most likely hypotheses are $J = 0$, 2, or 4[37]. Figure 23 shows the data taken in 1982 and 1983 separately. In parts (a) and (b) of the figure the masses are allowed to be different in the fits to the two data samples, and the fits show structures at different masses. If the mass is fixed to that seen in the 1983 data sample (see 23d), the fit of Figure 23c results. In order to confirm the ξ the Mark III collaboration hopes to obtain much more J/ψ data in the near future. It should be noted that DM2 at DCI has only reported upper limits on the ξ which are in mild conflict with the Mark III results[39].

The possible existence of a narrow resonance in this mass range in J/ψ radiative decays has stimulated speculation that the ξ might be a non-S-M Higgs boson[40], but at present more prosaic explanations[41] seem more likely.

Considerably more excitement was caused last summer by the announcement from the Crystal Ball collaboration of evidence for a narrow state in Υ radiative decays[42]. The large mass of the proposed state, called ζ, at 8.3 GeV/c^2, suggested to a number of theorists the possibility that the state was a non-S-M Higgs candidate[43]. The state was observed by the Crystal Ball in two independent final state configurations, one of higher multiplicity and hadronic character, and one of lower multiplicity possibly $\tau\bar{\tau}$.

Given the numerous reports on the ζ over the past six months, I will only briefly review the results presented at the summer conferences[42] as an orientation to presenting recent results from a run of about 200k Υ events taken by the Crystal Ball at DESY last Fall, and results from the CUSB detector also from a Fall run at CESR. These latest results are preliminary.

The first results came from a sample of about 100k $\Upsilon(1S)$ decays (10.4 pb^{-1}). Figure 24 shows the signal in the high multiplicity final state. The fit to the data, shown in the figure, yields a 4.2 s.d. effect at the ζ mass. Figure 25 shows the results from the low multiplicity final state. The fit to the data, shown in the figure, finds a 3.3 s.d. effect at a mass 10 MeV away from the fit in the high multiplicity case, and well within the statistical error on the mass measurement. Taken as independent, the two final state configurations yield a signal of over 5 s.d. The best estimate of the mass and width of the state is[42],

$$M_\zeta = (8.322 \pm 0.008 \pm 0.024)\ \text{GeV}/c^2\ ,$$

$$\Gamma < 80\ \text{MeV}\ (90\%\ \text{C.L.})\ . \qquad (25)$$

The branching ratio, $\Upsilon \to \gamma\zeta$, is somewhat model dependent since the manner in which the ζ decays can effect the efficiency for finding photons in the final state.

This is reflected in the product branching ratio into hadrons for the ς,

$$B[\Upsilon(1S) \rightarrow \gamma\varsigma] \times B[\varsigma \rightarrow \textit{hadrons}] = (0.47 \pm 0.11 \pm 0.26)\% \ , \qquad (26)$$

where the first error is statistical, and the second error is systematic with the bulk of this systematic error coming from uncertainties in the photon detection efficiency. Including the low multiplicity final state complicates matters even more, thus the Crystal Ball collaboration prefers to give the result as,

$$B[\Upsilon(1S) \rightarrow \gamma\varsigma] \sim 0.5\% \ . \qquad (27)$$

Given the excitement the announcement of the ς caused, it was natural that a large effort was mounted to check the initial report from the Crystal Ball. This was done both at DESY and Cornell last Fall. The Crystal Ball obtained about 200 k more Υ decays in the detector (22 pb^{-1}) in a six week run. The CUSB detector has obtained about 340 k more Υ decays in their detector (corresponding to about 22 pb^{-1} at CESR due to the narrower beam energy spread), making about 450 k events in total when adding in older data. In addition, 6 pb^{-1} were obtained at an energy just below the Υ in this run. CESR's run at the Υ continued for about 11 weeks. The results I report here for both detectors, essentially, have been reported previously[44,45].

In the interim between 1983 (100k Υ) and 1984 (200k Υ), the Crystal Ball detector underwent a major upgrade. A new tracking chamber system was installed which increased the number of proportional tube chamber layers from six to eight. Also, a new gas was used (Ar–CO_2–Methane), which stopped the chamber degradation with beam exposure which was previously plaguing the detector. This change necessitated a major restructuring of the online data acquisition hardware and software, and offline analysis software. These changes had been in progress for some time, but the Fall 1984 run was the first real physics data taken with the new system; of course there were problems in the

initial part of the run. The problems encountered only allowed a rapid analysis of the latter 60% of the data from this run, and only for the high multiplicity final state. Most of the first 40% of the data has been recovered and will be reported on soon for the high multiplicity channel. The low multiplicity channel is more problematic since the backgrounds in the analysis are sensitive to the tracking chamber quality (not the case for the high multiplicity analysis). Thus, the dramatic improvement of the new chamber system over the old one has necessitated a total rethinking of the charged particle cuts in the low multiplicity analysis. The Crystal Ball collaboration hopes that this analysis will be completed by this summer.

A comparison of the high multiplicity channel analysis from the 1983 run, 100k Υ, and the last 60% of the 1984 run, about 125k Υ, is presented in Figure 26a,b. The new data obviously do not confirm the ς. There is over a 4 s.d. difference at the ς mass between the 1983 data and this preliminary analysis of the last 60% of the 1984 data. The Crystal Ball collaboration does not presently understand the origin of this difference; however, the potential physics impact of the ς is so great that the experimenters have the burden of proof to show that the ς signal reproduces in every valid data set.

The CUSB collaboration has also reported new results. Their result at the Leipzig Conference[46] was an upper limit of 0.2% (90% C.L.) for the product branching ratio, $B[\Upsilon \rightarrow \gamma\varsigma] \times B[\varsigma \rightarrow hadrons]$. This result was based on a sample of 112k Υ decays. However, this upper limit is calculated using a photon efficiency based on a model of the QCD process, $\Upsilon \rightarrow \gamma gg$, for Υ radiative decay to the ς. If this model is used to obtain the branching ratio in the Crystal Ball (the 0.5% value in the Crystal Ball is obtained using a $c\bar{c}$ model for the hadronic decay of the ς[42]) the value obtained is about 0.25%. The new preliminary analysis from the CUSB collaboration, using the new data (340k decays) gives an upper limit for the product branching ratio of 0.14%-0.2% (90% C.L.)[45], depending on whether or not a new sector of the detector, made from BGO scintillator,

was included in the analysis or not (lower limit without BGO sector). The same model for Υ decays, $\Upsilon \rightarrow \gamma gg$, was used to calculate the photon efficiency, thus the CUSB upper limits are only in mild disagreement with the summer results[42] of the Crystal Ball. The most trouble for the ζ at this time is probably coming from the Crystal Ball itself.

The Search for Supersymmetric Particles

I report here recent limits obtained by the MAC collaboration[47] on the production of photinos $\tilde{\gamma}$ and sneutrinos $\tilde{\nu}$ in e^+e^- production at $E_{c.m.} = 29$ GeV . Figure 27 shows the diagrams tested for. The photino diagram has been calculated[48], and,

$$\sigma(e^+e^- \rightarrow \gamma\tilde{\gamma}\tilde{\gamma}) \sim \alpha^3 s/(M_{\tilde{e}})^4 \ . \tag{28}$$

Candidate events are selected by the size of their "perpendicular energy", $E_\perp$. All that is seen in the detector is a single photon candidate with,

$$E_\perp \geq (\sqrt{s} - E_\gamma) \sin\theta_{veto} \ , \tag{29}$$

where E_γ is the measured energy of the photon, and θ_{veto} is the minimum angle covered by the detector. Figure 28 shows the result of the search. Part (a) shows the observed $E_\perp$ spectrum for the first data sample taken (36 pb^{-1}), with $\theta_{veto} = 10^o$ and search region $E_\perp > 4.5$ GeV. Part (b) shows the observed $E_\perp$ spectrum for the second data sample taken (80 pb^{-1}), with $\theta_{veto} = 5^o$ and search region $E_\perp > 3.0$ GeV. One event is observed in the latter data sample. This result leads to the upper limit for photino production versus $\tilde{e}$ mass shown in part (c) of the figure. The experimental observations can also be turned into a limit on the sneutrino mass[47]. For $20 < M_{\tilde{W}} < 29$ GeV, $M_{\tilde{\nu}} > 10$ GeV/c^2.

Conclusions

1. The running of the coupling constant, α_s, predicted by QCD, is not presently seen by using measurements of R_{hadron}. However, the systematic errors on the measurements still allow a running α_s. It should be noted that when calculating α_s at the J/ψ and Υ using the technique of Lepage and Mackenzie[13], a running α_s is also not observed, but is allowed within error.

2. Evidence for the three gluon coupling predicted by QCD is still lacking. The search for gluonic mesons has continued to be inconclusive, even though candidate meson properties have been considerably refined.

3. Searches for right handed currents have so far proved negative, though impressive mass limits have been obtained. Searches for supersymmetric particles have also proved negative, with mass limits strongly coupled to accelerator energy. Much enthusiasm and inventiveness has been generated by the announcement of two possible new states, $\xi(2.2)$ and $\varsigma(8.3)$; however, the existence of these states is presently uncertain. In the case of the ς, theoretical interpretation outside the S-M played a very prominent role.

Acknowledgments

I would like to thank Michael Peskin for interesting and useful discussions. I also thank Alfred Fridman and Andreas Schwarz for useful suggestions and a careful reading of the manuscript. Finally, I would like to thank the organizers of the first of what I hope will be a long series of marvelous and stimulating conferences.

References

1. KOBAYASHI, M. & K. MASKAWA. 1973. Progr. Theor. Phys. 49: 652.

2. MAIANI, L. 1977, Proc. Int. Symp. on Lepton and Photon Interactions at High Energies, Hamburg 1977 (DESY, Hamburg 1977): 877.

3. UA1-COLLABORATION, ARNISON, G. *et al.* 1983. Phys. Rev. Lett. 122B:103. UA2-COLLABORATION, BANNER, M. *et al.* 1983. Phys. Lett. 122B: 476.

4. STROVINK, M. 1984. LBL-18231. BÙRAS, A. J. 1984. MPI-PAE/PTh 46184.

5. JADE-COLLABORATION, BARTEL, W. *et al.* 1979. Phys. Lett. 88B: 171; 136; 1980. Phys. Lett. 91B: 152; 1981. Phys. Lett. 100B: 364. 1983. Phys. Lett. 129B: 145.

6. MAC-COLLABORATION, FERNANDEZ, E. *et al.* 1984. SLAC-PUB-3479, submitted to Physical Review D.

7. For a nice review of the development of this theory using the notation used in this report see, C. KIESLING. 1984. *Recent Experimental Tests of the Standard Theory of Electroweak Interactions*, Habilitationsschrift, submitted to the Ludwig-Maximilians-Universität München.

8. DINE, M. & J. SAPIRSTEIN. 1979. Phys. Rev. Lett. 43: 668. CHETYRKIN, K. G., A. L. KATAEV & F.V. TKACHEV. 1979. Phys. Lett. 85B: 277. CELMASTER, W. & R. J. GONSALVES, 1978, Phys. Rev. Lett. 78: 132.

9. SCHWINGER, J., *Particles, Sources and Fields* (Addison-Wesley, New York, 1973), Vol. II, Chaps. 4 and 5. APPELQUIST, T. & H. D. POLITZER. 1975. Phys. Rev. Lett. 34: 43.

10. EDWARDS, C. *et al.* 1984. SLAC-PUB-3030.

11. MARK J-COLLABORATION, ADEVA, B. *et al.* 1983. MIT Report Number 131.

12. TASSO-COLLABORATION, BRANDELIK, R. *et al.* 1979. Phys. Lett. 83B: 261; 1980. Z. Phys. C; Particles and Fields, 4: 87; 1979. Phys. Lett. 88B: 199. 1982. Phys. Lett. 113B: 499.

13. MACKENZIE, P. B. & G. P. LEPAGE. 1981. Phys. Rev. Lett. 47: 1244.

14. Particle Properties Data Booklet. 1984. Rev. Mod. Phys. Vol. 56, No. 2, Part II.

15. APPELQUIST T. *et al.* 1978. Ann. Rev. Nucl. Part. Sci. 28: 387-499.

16. BLOOM, E. D. & C. W. Peck. 1983. Ann. Rev. Nucl. Part. Sci. 33: 143-197.

17. TUTS, P. M. 1983. Proc. Lepton Symposium, Cornell University, D. G. CASSEL & D. L. KREINICK, Eds.

18. CRYSTAL BALL COLLABORATION. 1985. SLAC-PUB-3575.

19. MOXHAY, P. & J. ROSNER. 1983. Phys. Rev. D28: 1132.

20. BAILLON, P. *et al.* 1967. Nuovo Cimento A50: 393.

21. EDWARDS, C. *et al.* 1982. Phys. Rev. Lett. 49: 259.

22. FRANKLIN, M. 1982. Ph.D. Thesis, SLAC-254; FRANKLIN, M. *et al.* 1983. Phys. Rev. Lett. 51: 963.

23. DIONISI, C. *et al.* 1980. Nucl. Phys. B169: 1.

24. MARK III-COLLABORATION, PERRIER, J. *et al.* 1984. SLAC-PUB-3436.

25. PROTOPOPESCU, S.D., 1984, Proc. of the Hadronic Session of the Nineteenth Rencontre de Moriond, La Plagne-Savoie-France, March 4-10, 1984. Vol. 2. New Particle Production: 689.

26. EDWARDS, C. 1984. Ph.D. Thesis, CALT-68-1165.

27. PERRIER, J., 1984, Invited talk presented at the Int. Conf. *Physics in Collision IV*, Santa Cruz, California, August 22-24, 1984. SLAC-PUB-3436.

28. EDWARDS, C. *et al.* 1982. Phys. Rev. Lett. 48: 458.

29. EINSWEILER, K. F. 1984. Ph.D. Thesis, SLAC-272.

30. AUGUSTIN, J. E. *et al.* 1984, Contributed paper to the XXII Int. Conf. on High Energy Physics, Leipzig, July 19-25, 1984.

31. BLOOM, E.D., 1982, Invited talk presented at 21st Int. Conf. on High Energy Physics, Paris, France, July 26-31. C3: 407, J. Phys. C3, Suppl. 12.

32. BISTIRLICH, J., BOSSINGHAM, R., CHACON, A., CLAWSON, C., CROWE, K., HUMANIC, T., MARTOFF, C., & MEYER, C. (LBL/University of California, Berkeley); JANSEN, J. (SIN); BREWER, J., KEITEL, R., ORAM, C. & SALOMON, M. (University of British Columbia/TRIUMF).

33. BALKE, B., CARR, B., GIDAL, G., JODIDIO, A., SHINSKY, K. A. (deceased), STEINER, H. M., STOKER, D. P., STROVINK, R. D., & TRIPP M. (LBL/University of California, Berkeley); GOBBI, B. (Northwestern); ORAM, C. J. (TRIUMF).

34. STROVINK, M. 1984, Rapporteur talk presented at XIth Int. Conf. on Neutrino Physics and Astrophysics, Nordkirchen near Dortmund, FRG. LBL Report #18231.

35. SCHECK, F. 1978. Phys. Report 44C: 187.

36. ABRAMOWICZ, H. *et al.* 1982. Z. Phys. C12: 225.

37. MARK III-COLLABORATION, EINSWEILER, K. 1983. SLAC-PUB-3202; presented at the Int. Europhysics Conf. on HEP, Brighton, England, July 20-27.

38. PARTRIDGE, R. 1984. Talk at this conference.

39. AUGUSTIN, J. E. *et al.* 1984, Contributed paper to the XXII Int. Conf. on High Energy Physics, Leipzig, July 19-25, 1984.

40. HABER, H. E. & G. L. KANE. 1984. Phys. Lett. 135B: 196.

41. GODFREY, S. *et al.* 1984. Phys. Lett. 141B: 439.

42. CRYSTAL BALL COLLABORATION, PECK, C. 1984. SLAC-PUB-3380 and DESY 84-064; TROST, H. 1984, Contributed paper to the XXII Int. Conf. on High Energy Physics, Leipzig, July 19-25; NICZYPORUK, B. 1984, SLAC Summer Institute on Particle Physics, July 23-August 3; COYNE, D. G. 1984, Invited talk presented at the Conf. on Physics in Collision IV, University of Santa Cruz, Santa Cruz, California.

43. GLASHOW, S. L. & M. MACHACEK. 1984. Phys. Lett. 145B: 302. PHAM, X. 1984. PAR/LPTHE-84/38. TU, T. 1984. BIHEP-TH-84-22. GLÜCK, M. 1984. DO-TH-84/23. SHIU, M. *et al.* 1984. HUTP-84/A068. GEORGI, H. *et al.* 1984. Phys. Lett. 149B: 234. RODENBERG, R. 1984. print-84-0843 (AACHEN). LANE, K. *et al.* 1984. DOE-ER-1545-352 & NSF-ITP-84-116. NANDI, S. 1984. DOE-ER-03992-563 (Texas). HABER, H. E. & G. L. KANE. 1984. UM TH 84-26. CLAVELLI, L. *et al.* 1984. IUHET-96a. PANTALEONE, Z. *et al.* 1984. SLAC-PUB-3439. WU, DAN–DI. 1984. KFK-TH 97.

44. CRYSTAL BALL COLLABORATION, BROCK, I. 1984. To be published in the Proc. of the Meeting of the American Physical Society, Dept. of Particles and Fields, Santa Fe, New Mexico, October 31-November 3.

45. CUSB-COLLABORATION, TUTS, M. 1984. To be published in the Proc. of the Meeting of the American Physical Society, Dept. of Particles and Fields, Santa Fe, New Mexico, October 31-November 3.

46. CUSB-COLLABORATION, FRANZINI, P. 1984. Question and Answer Period, Leipzig Meeting, & private communication.

47. MAC-COLLABORATION. 1985. Phys. Rev. Lett. 54: 95.

48. WARE, J. & M. E. MACHACEK. 1984. Phys. Lett. 142B: 300. KOBAYASHI, T. & M. KURODA. 1984. Phys. Lett. 139B: 208. GRASSIE, K. & P. N. PANDITA. 1984. Phys. Rev. D30: 22.

49. LENA COLLABORATION, NICZYPORUK, B. *et al.* 1982. Z. Phys. C15: 299.

Table 1. α_s from various sources.

$(\sqrt{s})_{effective}$(GeV)	α_s^{Theory}	$\alpha_s^{\text{Experiment}}$	Comments
4.54	—	0.165 ± 0.005	Υ decay, (14)
6	0.155	0.12 ± 0.11	R, CB, (10)
29	0.125	0.23 ± 0.06	R, No electroweak included, MAC, (6)
32	0.123	~ 0.20	R, $\sin^2\theta_W = 0.23$, JADE, (5)
32	0.123	~ 0.18	R, $\sin^2\theta_W = 0.23$, TASSO, (12)

Table 2. Experimental determination of hadronic width of 1^3P_J states.

State	System	Γ_{had}(MeV)	Comments
$^3P_0$	$c\bar{c}$	17 ± 3.5	CB, (16)
$^3P_1$	$c\bar{c}$	$< 3.8(90\%CL)$	CB, (16)
$^3P_2$	$c\bar{c}$	2.9 ± 2	CB, (16)
$^3P_1$	$b\bar{b}$	$0.041^{+0.04}_{-0.02}$	CUSB, (17)
$^3P_2$	$b\bar{b}$	$0.152^{+0.063}_{-0.050}$	CUSB, (17)
$^3P_1$	$b\bar{b}$	$0.079^{+0.029}_{-0.019}$	CB, (18)
$^3P_2$	$b\bar{b}$	$0.101^{+0.045}_{-0.028}$	CB, (18)

Figure Captions

Figure 1. The quark mixing matrix in the Kobayashi-Maskawa and Maiani forms. c_i and s_i denote $\cos\theta_i$ and $\sin\theta_i$ respectively.

Figure 2. The various types of interactions seen from an e^+e^- initial state. Many of these reactions are serious backgrounds to R_{hadron} (the upper right cubby).

Figure 3. The generic R_{hadron} detector as illustrated by the Crystal Ball detector.

Figure 4. Comparison, in the MAC detector, of data (solid circles) and Monte Carlo (histogram) for distributions of transverse energy, E_t, and energy asymmetry, I.

Figure 5. Comparison, in the Crystal Ball detector, of energy asymmetry for (a) cosmic rays, (b) Monte Carlo hadrons at $\sqrt{s} = 5$ GeV.

Figure 6. The ratio of large angle luminosity measurements to small angle in the Crystal Ball detector. The open circles are 1980 data, the closed circles 1981 data.

Figure 7. R_{hadron} for selected measurements with the overall systematic error $\pm 7\%$. The references to the various measurements are given in the text, except for LENA[49].

Figure 8. Same as for Figure 7, except lines at $R_{hadron} = 3.333$ and 3.667, from simple parton model shown for reference.

Figure 9. R_{hadron} from TASSO and Mark J compared to full electroweak theory and ranges of $\sin\theta_W$.

Figure 10. $R_{(QCD+WEAK)}/R_{QCD}$ vs. $\sin^2\theta_W$, for $\sqrt{s} = 14$, 35 GeV.

Figure 11. Lowest order diagram from QCD yielding $\Gamma_{had}(^3P_0)$ and $\Gamma_{had}(^3P_2)$.

Figure 12. a) Gluon gluon interaction via gluon exchange predicted by QCD. b) possible gluonic meson production mechanism in quarkonium decays.

Figure 13. Experimental status of ι. a) Crystal Ball results, b), c) Mark III results, table summarizing status.

Figure 14. Results on $J/\psi \to \gamma\gamma\rho$. a) Mark III, b) Crystal Ball, c) DM2, table summarizing extraction of $\gamma\rho$ contribution at ι mass. The results in the table might correspond to an ι contribution, based on a spin analysis .

Figure 15. Results from 1982 on the $\theta(1700)$. a) $\eta\eta$ final state, b) K^+K^- final state, c) no signal seen in $\pi^+\pi^-$ final state, d) no signal seen in $\pi^0\pi^0$ final state.

Figure 16. Present experimental status of $\theta(1700)$. a) Mark III K^+K^- final state, b) Mark III $\pi^+\pi^-$ final state with signal evident.

Figure 17. a) The CUSB inclusive prompt photon spectrum from the $\Upsilon(1S)$, b) the Mark II inclusive prompt photon energy spectrum from the J/ψ, c) the Crystal Ball inclusive (unsubtracted) photon energy spectrum from the J/ψ.

Figure 18. Muon decay via (V−A). Angular momentum conservation forces the decay rate to zero for positrons decaying backward relative to the muon spin direction. The presence of a (V+A) component allows such a backward decay.

Figure 19. a) The positron momentum spectrum from μ^+ decay at rest used by the B-S-T group in their preliminary determination of the decay parameter η, b) the μSR asymmetry measured by the B-N-S group in their preliminary determination of the muon decay parameter δ.

Figure 20. Distributions in reduced positron momentum, x, with the spin (a) precessed due to the presence of a 70 or 120 Gauss tranverse field, (b) 1.1 T parallel field. (c) Fitted $(\xi P_\mu \delta/\rho)\cos\theta$ for data like those in (b), divided into bins of $\cos\theta$. (d) The decay time spectrum for data with transverse field [as in (a)] with muon lifetime factored out.

Figure 21. Experimental 90%-C.L. limits in the $\alpha - \varsigma$ plane for the B-N-S experiment, shaded area, and CDHS, region interior to bold lines.

Figure 22. Mark III results for $J/\psi \to \gamma\xi$, $\xi \to K^+K^-$. a) 1982 data alone, b) 1983+1982 data combined.

Figure 23. Mark III $\xi(2.2)$ results continued. a) 1982, b) 1983, results fitted allowing the mass of the resonance to vary in the fit. c) 1982, d) 1983, results fitted keeping the resonance mass fixed at the 1983 value.

Figure 24. Crystal Ball results for $\Upsilon(1S) \to \gamma\varsigma(8.3)$, $\varsigma \to$ *hadrons*. a) The inclusive photon spectrum after all cuts including physics-oriented cuts, b) the region of the ς peak of (a), with fit shown as a solid line, c) same as (b) with the fitted background subtracted.

Figure 25. Crystal Ball results for $\Upsilon(1S) \to \gamma\varsigma(8.3)$, $\varsigma \to$ low multiplicity, $\tau^+\tau^-$ biased sample including all cuts. a) The inclusive photon spectrum, b) the ς peak region of (a), with fit shown as a solid line, c) the same as (b) with fitted background subtracted.

Figure 26. Crystal Ball results for $\Upsilon(1S) \to \gamma\varsigma(8.3)$, $\varsigma \to$ multihadrons. a) The results from 1983 data shown already in 24a (100k Υ decays), b) the preliminary results from 1984 data, no ς peak is seen (125 k Υ decays).

Figure 27. Diagrams used to calculate a) $e^+e^- \to \gamma\tilde{\gamma}\tilde{\gamma}$; b) and c) $e^+e^- \to \gamma\tilde{\nu}\tilde{\nu}$.

Figure 28. Results from the MAC collaboration on $\tilde{\gamma}$ production. a) The observed $E_\perp$ spectrum for the first data sample of 36 pb^{-1} with $\theta_{veto} = 10^0$ and search region $E_\perp > 4.5$ GeV, b) the spectrum for the second data sample of 80 pb^{-1} with $\theta_{veto} = 5^0$ and search region $E_\perp > 3.0$ GeV, c) the lower limit for $M_{\tilde{e}}$ as a function of $M_{\tilde{\gamma}}$; the solid curve is for $M_{\tilde{e}_L} = M_{\tilde{e}_R}$; the dashed curve for $M_{\tilde{e}_L} \gg M_{\tilde{e}_R}$; the limits are at 90% C.L.

Kobayashi – Maskawa

$$\begin{array}{c} \\ u \\ c \\ t \end{array} \begin{array}{c} \begin{array}{ccc} d & s & b \end{array} \\ \begin{pmatrix} c_1 & s_1 c_3 & s_1 s_3 \\ -s_1 c_2 & c_1 c_2 c_3 - e^{i\delta} s_2 s_3 & c_1 c_2 s_3 + e^{i\delta} s_2 c_3 \\ s_1 s_2 & -c_1 s_2 c_3 - e^{i\delta} c_2 s_3 & -c_1 s_2 s_3 + e^{i\delta} c_2 c_3 \end{pmatrix} \end{array}$$

Maiani

$$\begin{array}{c} \\ u \\ c \\ t \end{array} \begin{array}{c} \\ \begin{pmatrix} c_\beta c_\theta & c_\beta s_\theta & s_\beta \\ -s_\gamma c_\theta s_\beta e^{i\delta'} - s_\theta c_\gamma & c_\gamma c_\theta - s_\gamma s_\beta s_\theta e^{i\delta'} & s_\gamma c_\beta e^{i\delta'} \\ -s_\beta c_\gamma c_\theta + s_\gamma s_\theta e^{-i\delta'} & -c_\gamma s_\beta s_\theta - s_\gamma c_\theta e^{-i\delta'} & c_\gamma c_\beta \end{pmatrix} \end{array}$$

1-85

5031A1

Fig. 1

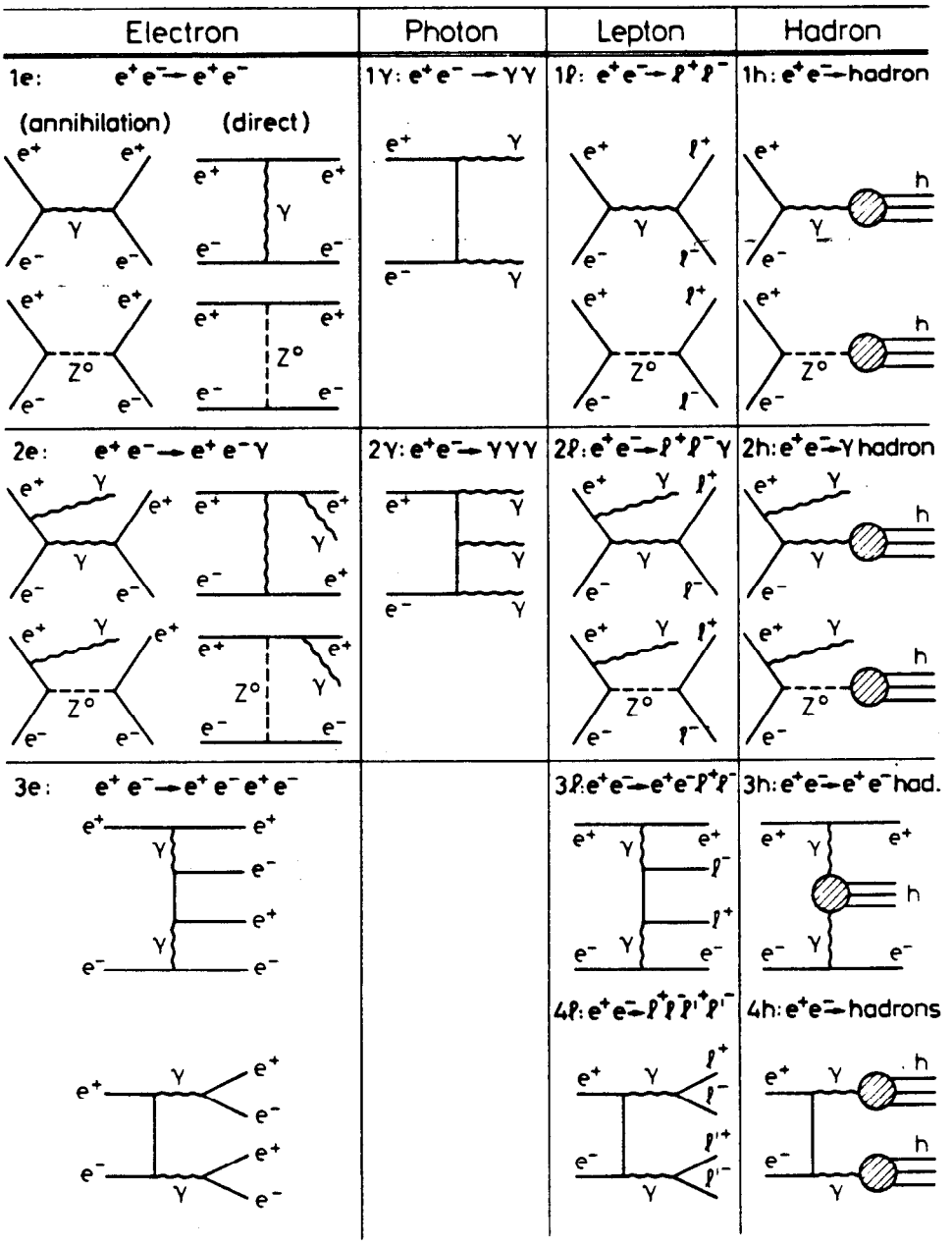

2-85

5031A2

Fig. 2

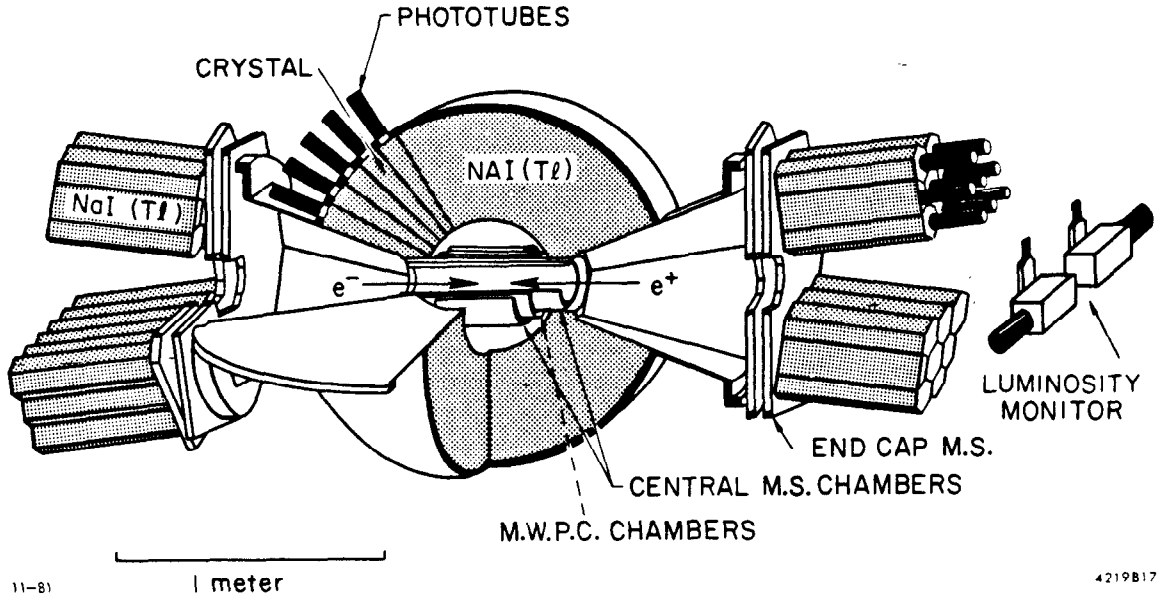
PHOTOTUBES
CRYSTAL
NAI (Tℓ)
NaI (Tℓ)
e⁻
e⁺
LUMINOSITY MONITOR
END CAP M.S.
CENTRAL M.S. CHAMBERS
M.W.P.C. CHAMBERS
1 meter
11-81
4219B17

Fig. 3

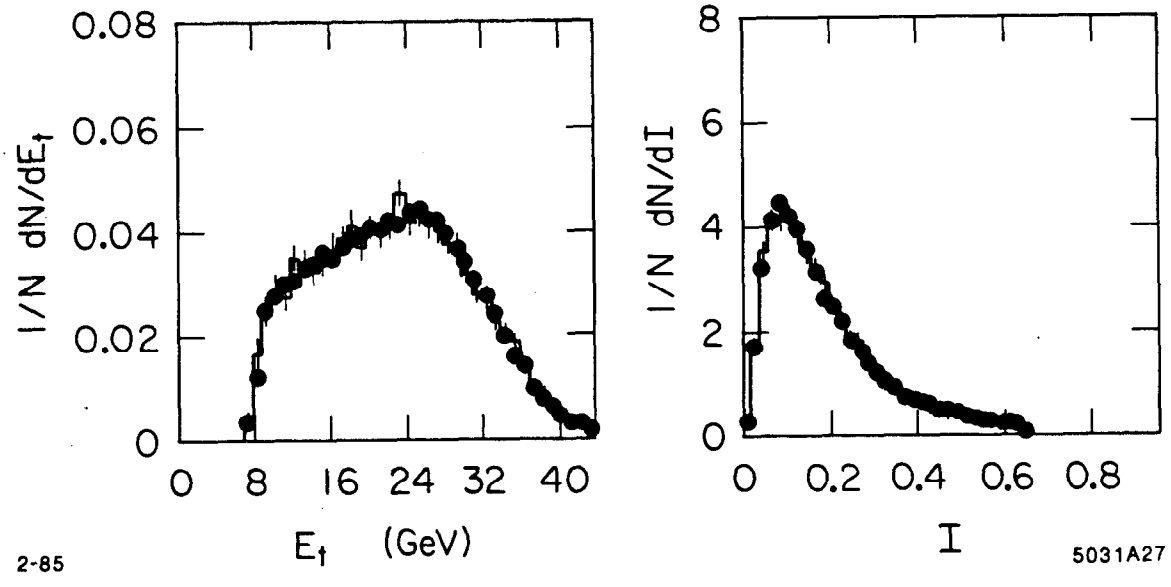
0.08
0.06
0.04
0.02
0
1/N dN/dE_t
0 8 16 24 32 40
E_t (GeV)
8
6
4
2
0
1/N dN/dI
0 0.2 0.4 0.6 0.8
I
2-85
5031A27

Fig. 4

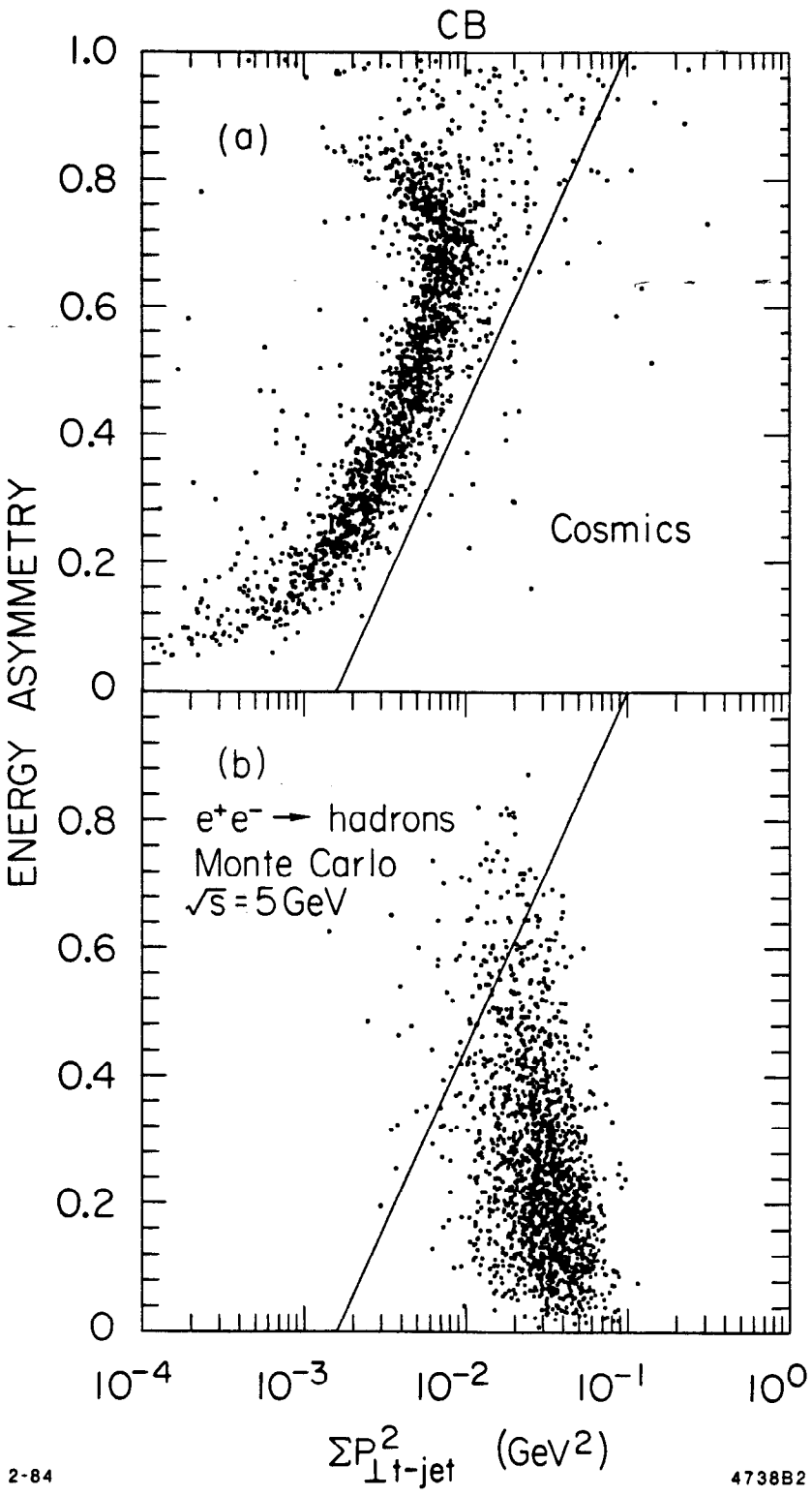
CB
(a)
Cosmics
(b)
e+e− → hadrons
Monte Carlo
√s = 5 GeV
ENERGY ASYMMETRY
1.0
0.8
0.6
0.4
0.2
0
10−4
10−3
10−2
10−1
10^0
ΣP²⊥t-jet (GeV²)
2-84
4738B2

Fig. 5

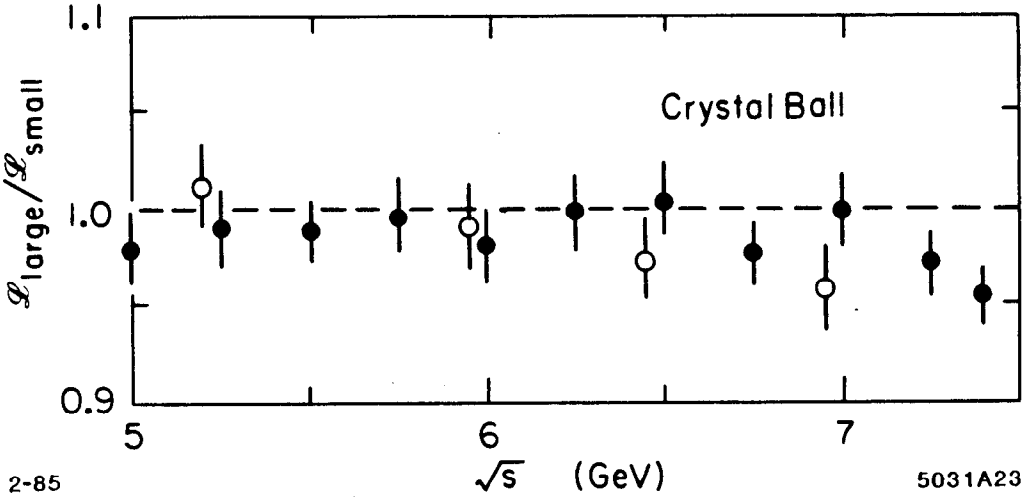
1.1
1.0
0.9
$\mathscr{L}_{large}/\mathscr{L}_{small}$
Crystal Ball
5
6
7
$\sqrt{s}$ (GeV)
2-85
5031A23

Fig. 6

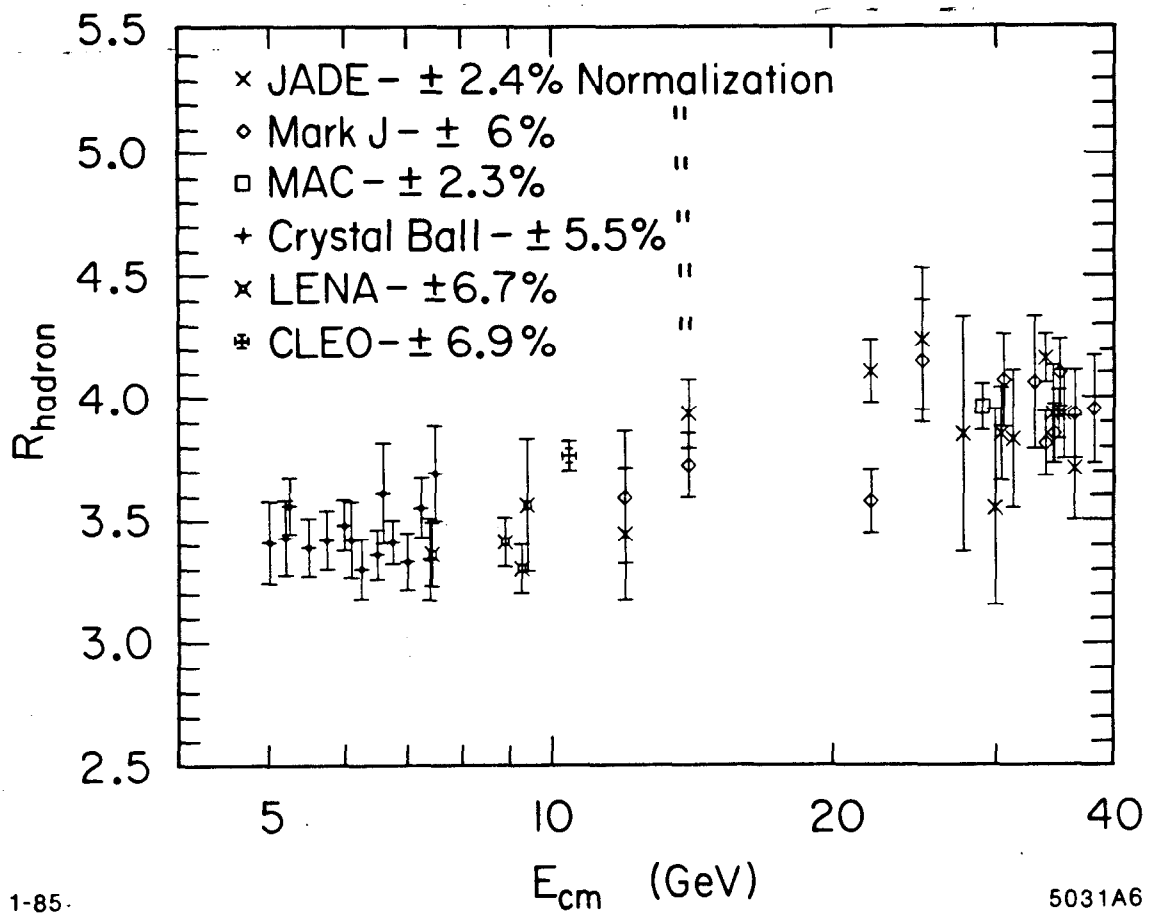
× JADE – ± 2.4% Normalization
◇ Mark J – ± 6%
□ MAC – ± 2.3%
+ Crystal Ball – ± 5.5%
× LENA – ±6.7%
CLEO – ± 6.9%
R hadron
5.5
5.0
4.5
4.0
3.5
3.0
2.5
5
10
20
40
E cm (GeV)
1-85
5031A6

Fig. 7

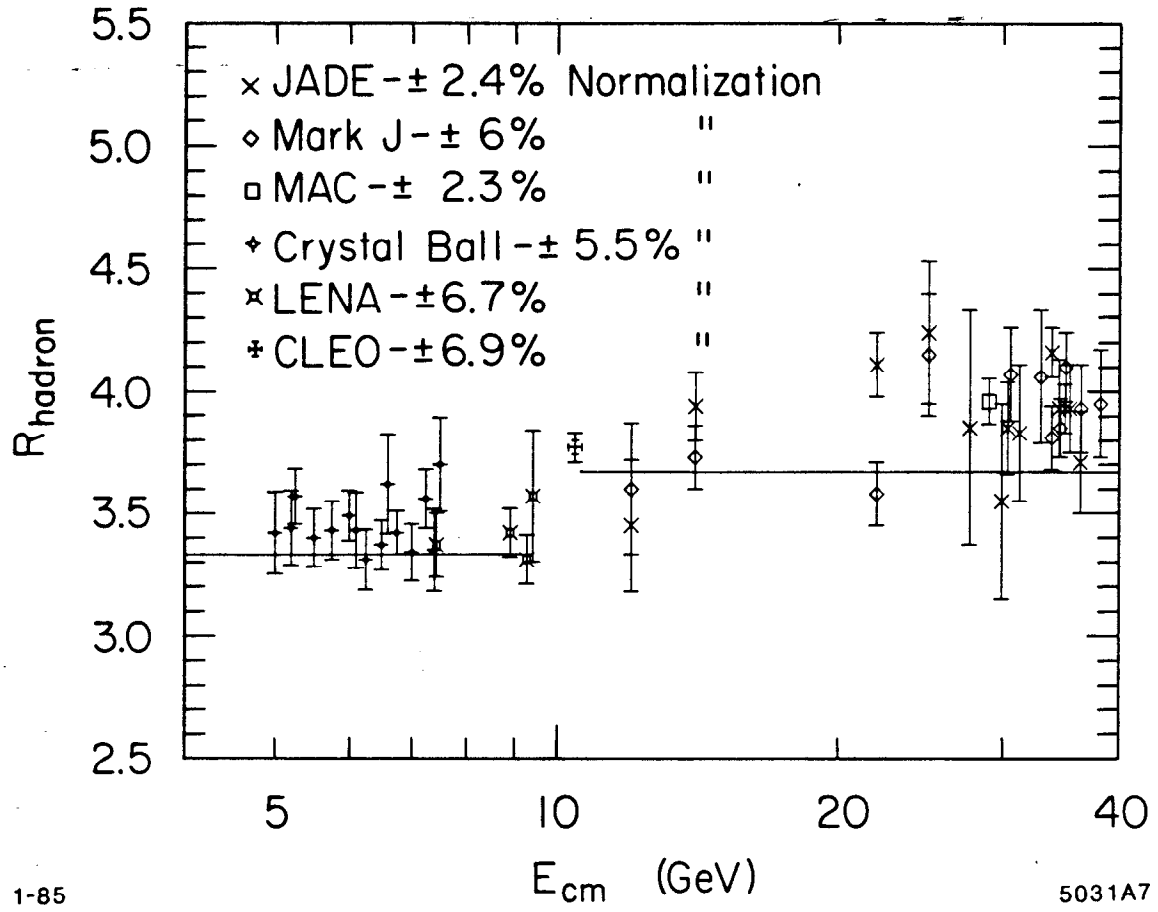
× JADE - ± 2.4% Normalization
◇ Mark J - ± 6% "
□ MAC - ± 2.3% "
✦ Crystal Ball - ± 5.5% "
⋆ LENA - ± 6.7% "
+ CLEO - ± 6.9% "
R_{hadron}
5.5
5.0
4.5
4.0
3.5
3.0
2.5
5
10
20
40
E_{cm} (GeV)
1-85
5031A7

Fig. 8

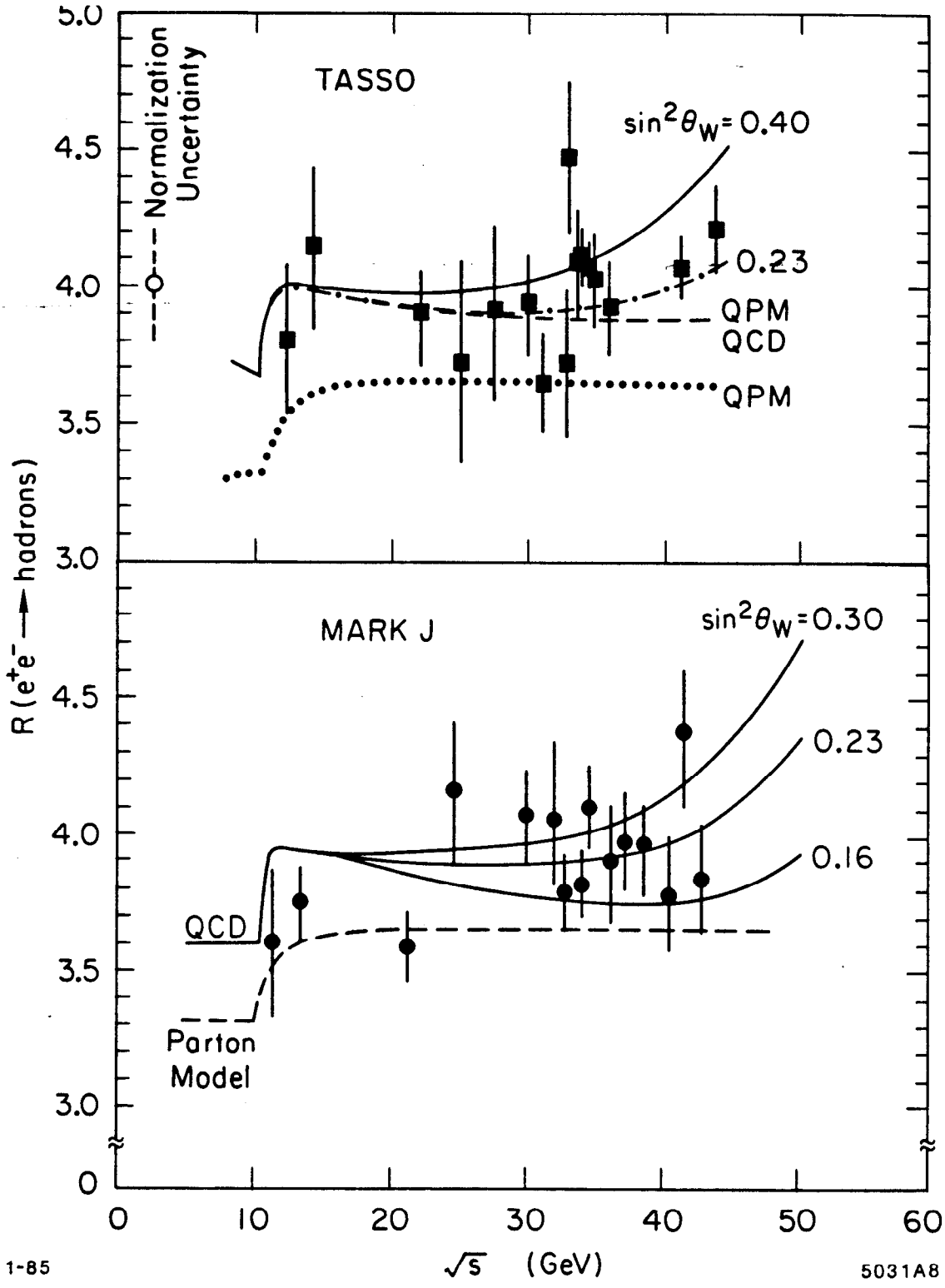
TASSO
Normalization Uncertainty
$\sin^2\theta_W = 0.40$
0.23
QPM
QCD
QPM
MARK J
$\sin^2\theta_W = 0.30$
0.23
0.16
QCD
Parton Model
R (e^+e^- → hadrons)
$\sqrt{s}$ (GeV)
1-85
5031A8

Fig. 9

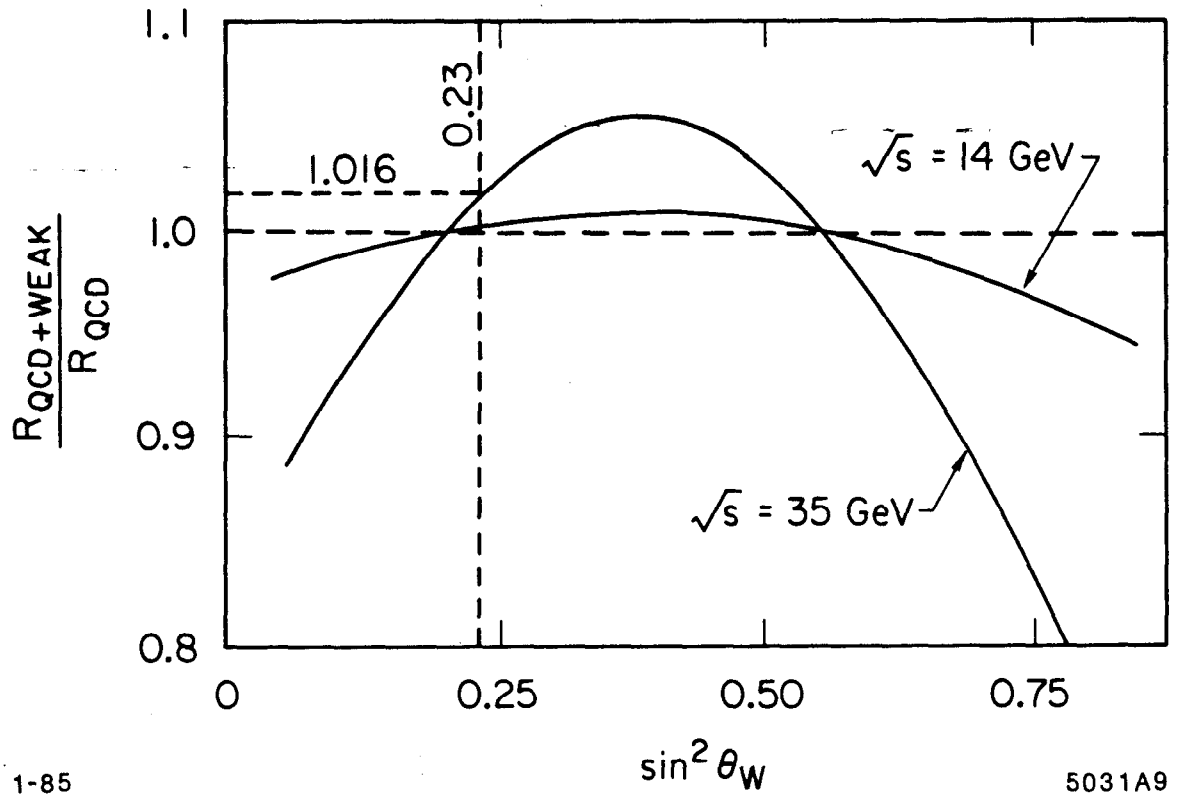
1.1
1.0
0.9
0.8
0
0.25
0.50
0.75
0.23
1.016
$\sqrt{s}$ = 14 GeV
$\sqrt{s}$ = 35 GeV
$\frac{R_{QCD+WEAK}}{R_{QCD}}$
$\sin^2\theta_W$
1-85
5031A9

Fig. 10

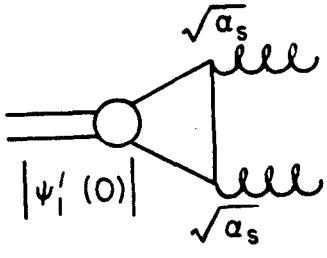

1-85 5031A10

Fig. 11

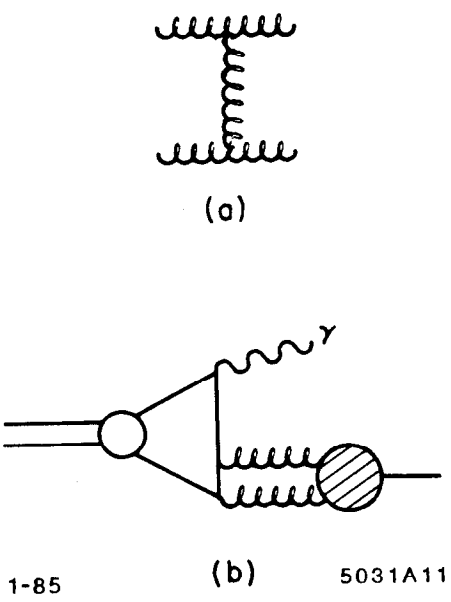

Fig. 12

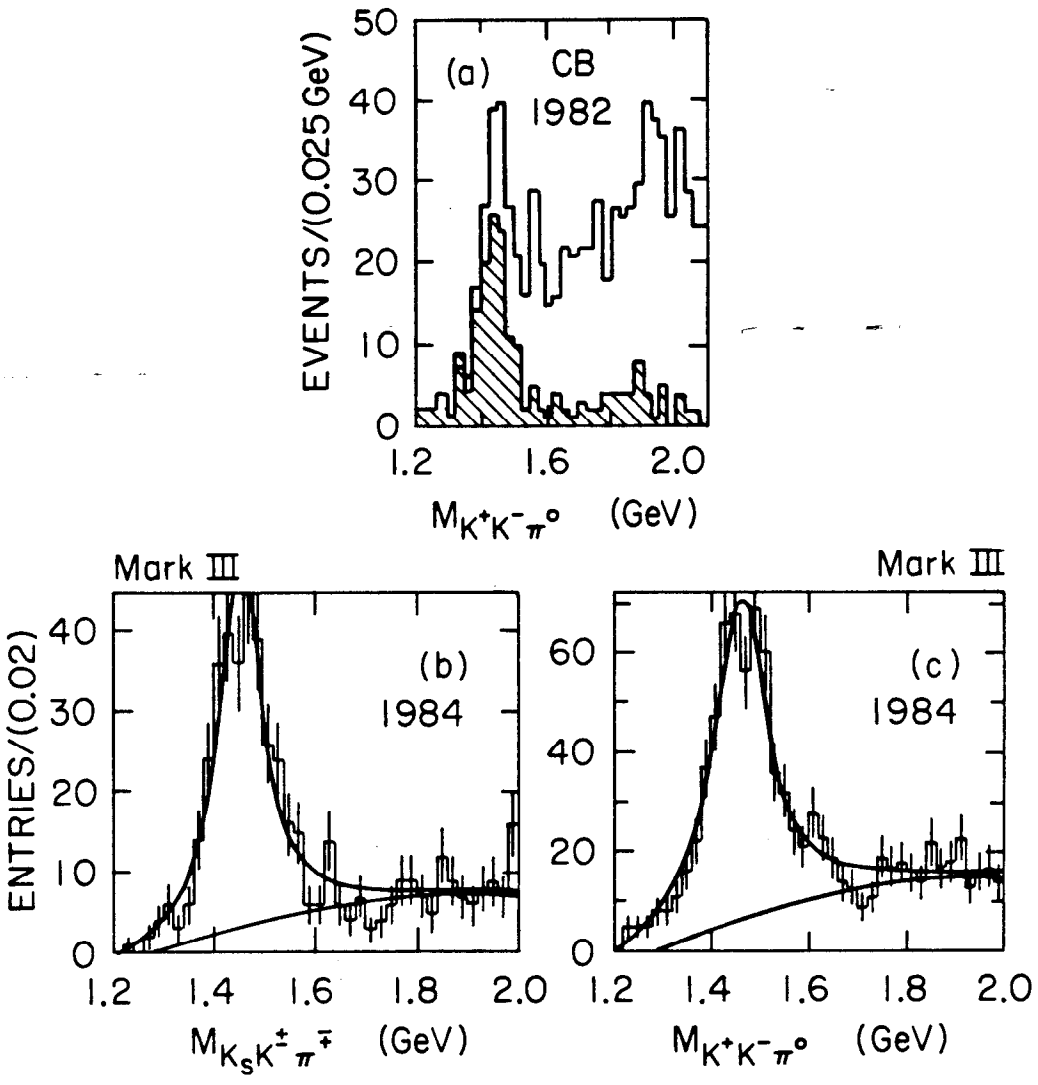

$\iota(1440)$ present experimental status.

Collaboration	Decay Mode	Mass (MeV)	Width (MeV)	$B(J/\psi \to \gamma\iota) \times B(\iota \to K\bar{K}\pi)$	J^{P+}
Mark II	$K_SK^\pm\pi^\mp$	1440^{+10}_{-15}	50^{+30}_{-20}	$(4.3 \pm 1.7) \times 10^{-3}$	
Crystal Ball	$K^+K^-\pi^o$	1440^{+20}_{-15}	55^{+20}_{-30}	$(4.0 \pm 0.7 \pm 1.0) \times 10^{-3}$	0^-
Mark III	$K_SK^\pm\pi^\mp$	1456 ± 10	95 ± 7	$(5.0 \pm 0.5 \pm 0.7) \times 10^{-3}$	0^-
	$K^+K^-\pi^o$	1460 ± 10	103 ± 10		
DM2	$K_SK^\pm\pi^\mp$	1474 ± 15	76 ± 16		

2-85 5031A25

Fig. 13

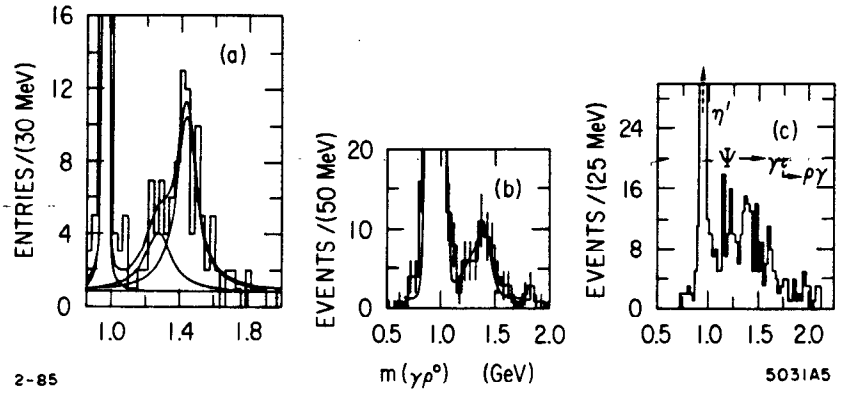

$J/\psi \to \gamma X(1400)$, $X(1400) \to \gamma\rho^o$ branching ratio. The mass and width of the 1400 MeV structure were respectively fixed at 1440 MeV and 55 MeV in the Crystal Ball fit.

Collaboration	$B(J/\psi \to \gamma X(1400))$ $\times B(X(1400) \to \gamma\rho^o)$
Crystal Ball	$(0.88 \pm 0.28 \pm 0.15) \times 10^{-4}$
Mark III	$(1.1 \pm 0.24 \pm 0.25) \times 10^{-4}$

Fig. 14

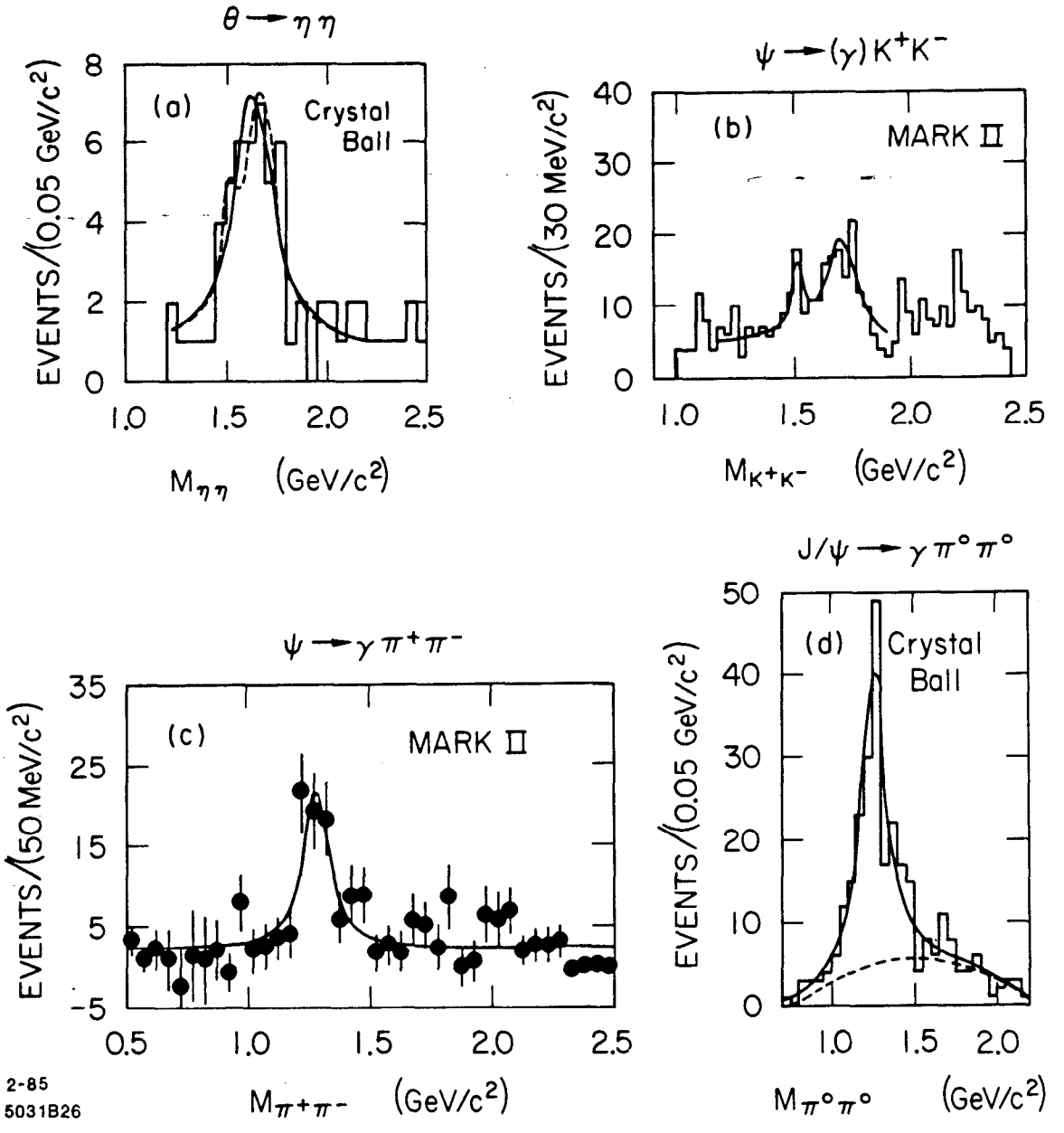
θ → ηη
(a)
Crystal Ball
EVENTS/(0.05 GeV/c²)
Mηη (GeV/c²)
ψ → (γ) K⁺K⁻
(b)
MARK II
EVENTS/(30 MeV/c²)
MK⁺K⁻ (GeV/c²)
ψ → γ π⁺π⁻
(c)
MARK II
EVENTS/(50 MeV/c²)
Mπ⁺π⁻ (GeV/c²)
J/ψ → γ π°π°
(d)
Crystal Ball
EVENTS/(0.05 GeV/c²)
Mπ°π° (GeV/c²)
2-85
5031B26

Fig. 15

$\theta(1690)$ present experimental status. Upper limits are given at the 90% confidence level.

Collaboration	Decay Mode	Mass (MeV)	Width (MeV)	$B(\psi \to \gamma\theta) \times B(\theta \to X)$	J^P
Crystal Ball	$\eta\eta$	1670 ± 50	160 ± 80	$(3.8 \pm 1.6) \times 10^{-4}$	2^+ (95% CL)
	$\eta\eta'$			$< 2.1 \times 10^{-4}$	
	$\pi\pi$			$< 6 \times 10^{-4}$	
Mark III	K^+K^-	1720 ± 10	130 ± 20	$(4.8 \pm 0.6 \pm 0.9) \times 10^{-4}$	2^+ (99.9% CL)
	$\pi^+\pi^-$	1713 ± 15	—	$(1.6 \pm 0.4 \pm 0.3) \times 10^{-4}$	
	$\rho^o\rho^o$			$< 2.0 \times 10^{-4}$	
	$K\bar{K}\pi$			$< 2.5 \times 10^{-4}$	
	$K^+K^-\pi^+\pi^-$			$< 1.0 \times 10^{-4}$	
Mark II	K^+K^-	1708 ± 30	156 ± 60	$(6.0 \pm 0.9 \pm 2.5) \times 10^{-4}$	2^+ (80% CL)
	$\pi\pi$			$< 3.2 \times 10^{-4}$	
DM2	K^+K^-	1718 ± 29	233 ± 75		

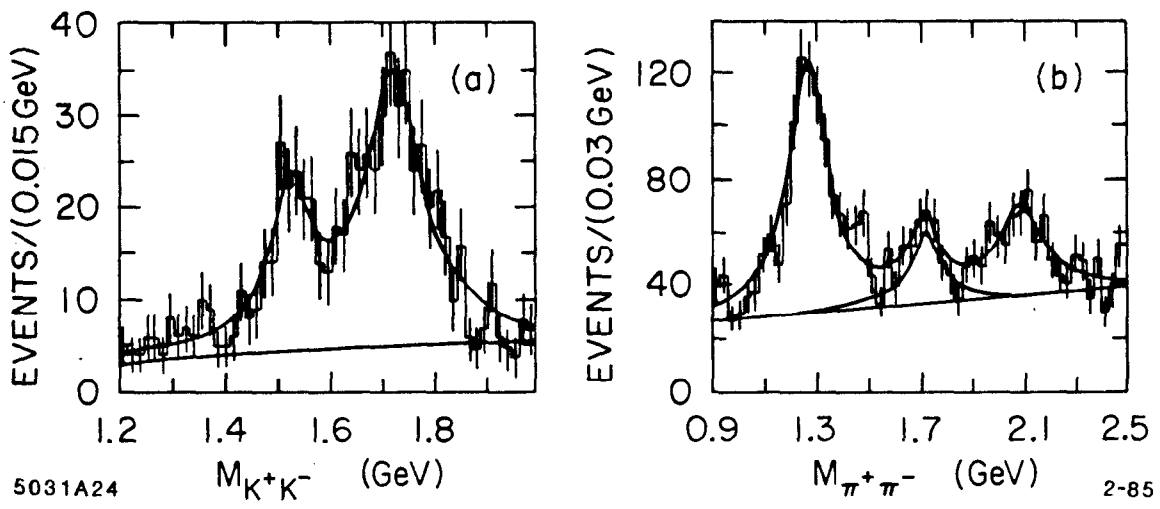

Fig. 16

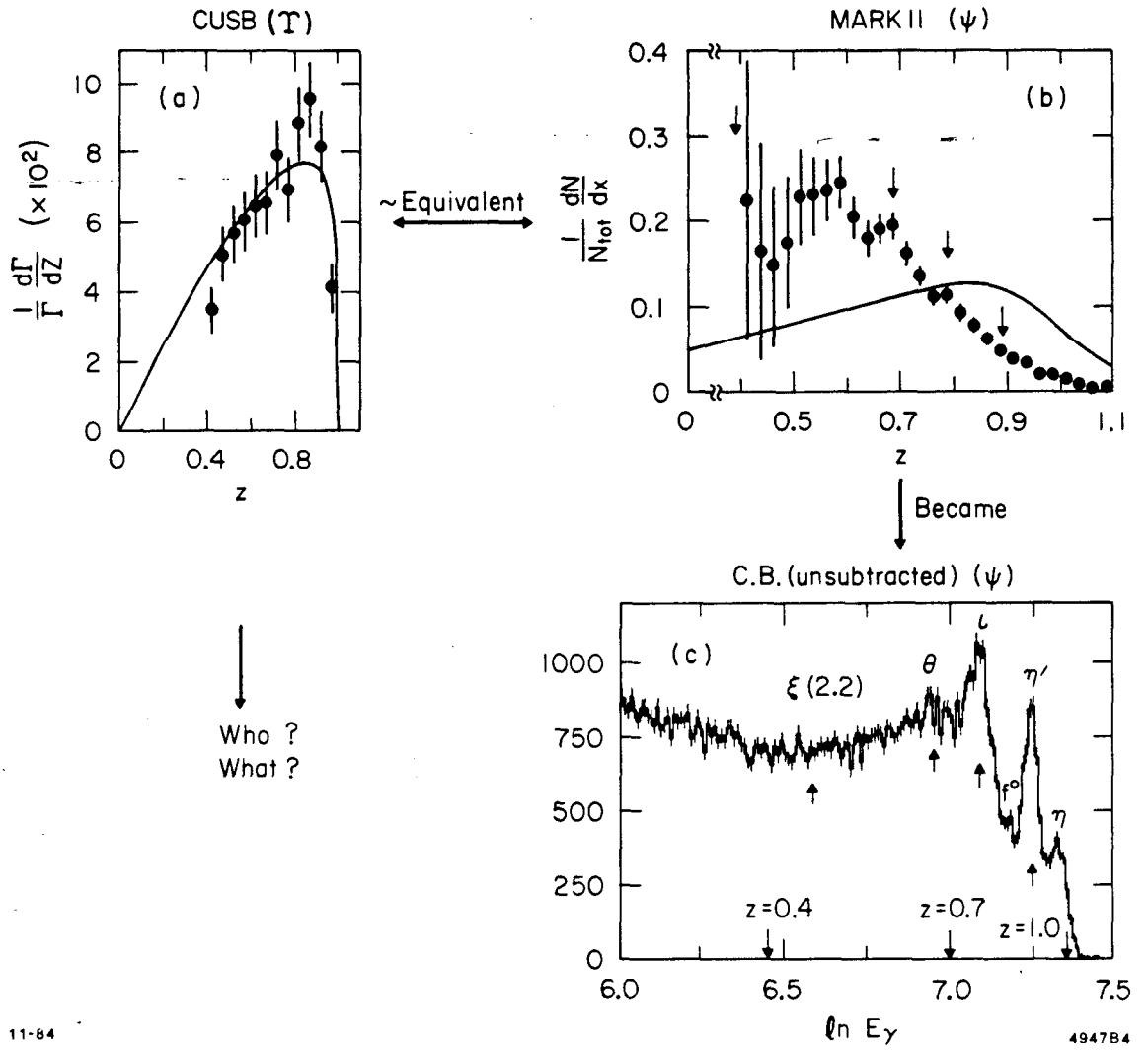
CUSB (Υ)
(a)
$\frac{1}{\Gamma}\frac{d\Gamma}{dZ}$ (x 10²)
z
~Equivalent
MARK II (ψ)
(b)
$\frac{1}{N_{tot}}\frac{dN}{dx}$
z
Became
C.B. (unsubtracted) (ψ)
(c)
ξ (2.2)
θ
ι
η′
f°
η
z=0.4
z=0.7
z=1.0
ℓn E_γ
Who ?
What ?
11-84
4947B4

Fig. 17

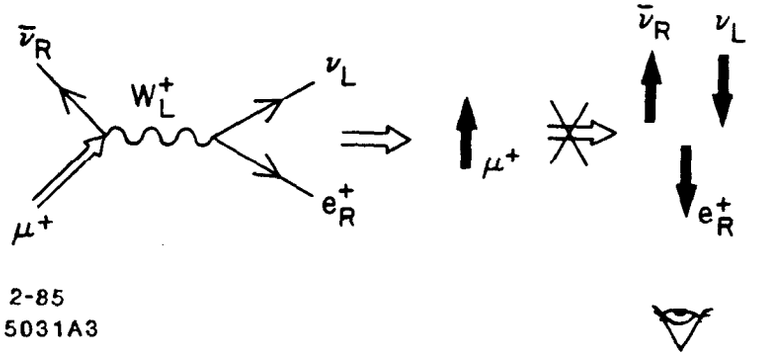

Fig. 18

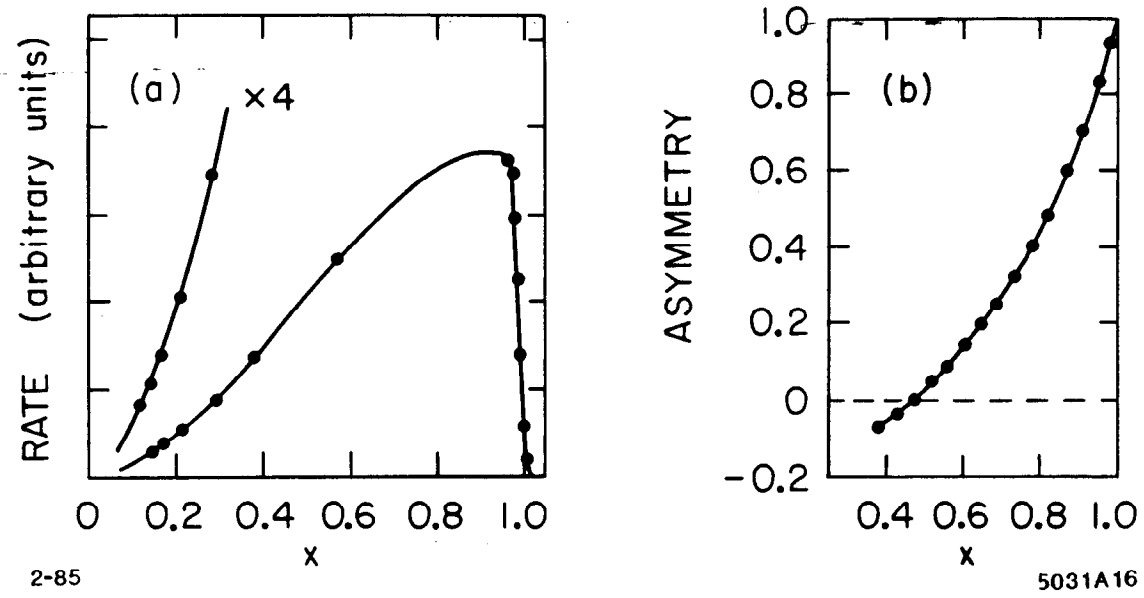
RATE (arbitrary units)
(a)
×4
0
0.2
0.4
0.6
0.8
1.0
x
2-85
ASYMMETRY
(b)
1.0
0.8
0.6
0.4
0.2
0
-0.2
0.4
0.6
0.8
1.0
x
5031A16

Fig. 19

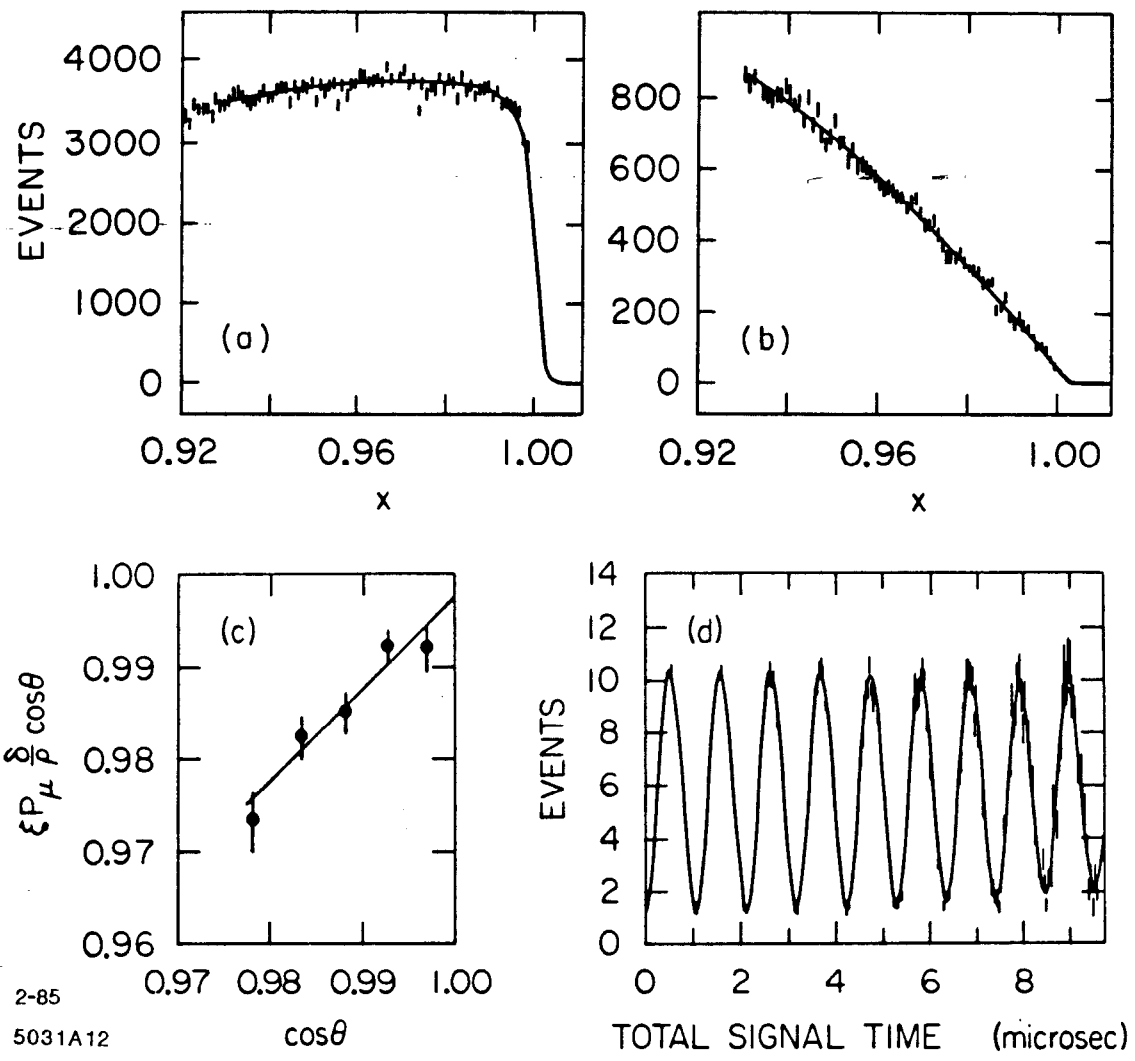
4000
3000
2000
1000
0
EVENTS
(a)
0.92
0.96
1.00
x
800
600
400
200
0
(b)
0.92
0.96
1.00
x
1.00
0.99
0.98
0.97
0.96
$\xi P_\mu \frac{\delta}{\rho} \cos\theta$
(c)
0.97
0.98
0.99
1.00
cosθ
2-85
5031A12
14
12
10
8
6
4
2
0
EVENTS
(d)
0
2
4
6
8
TOTAL SIGNAL TIME (microsec)

Fig. 20

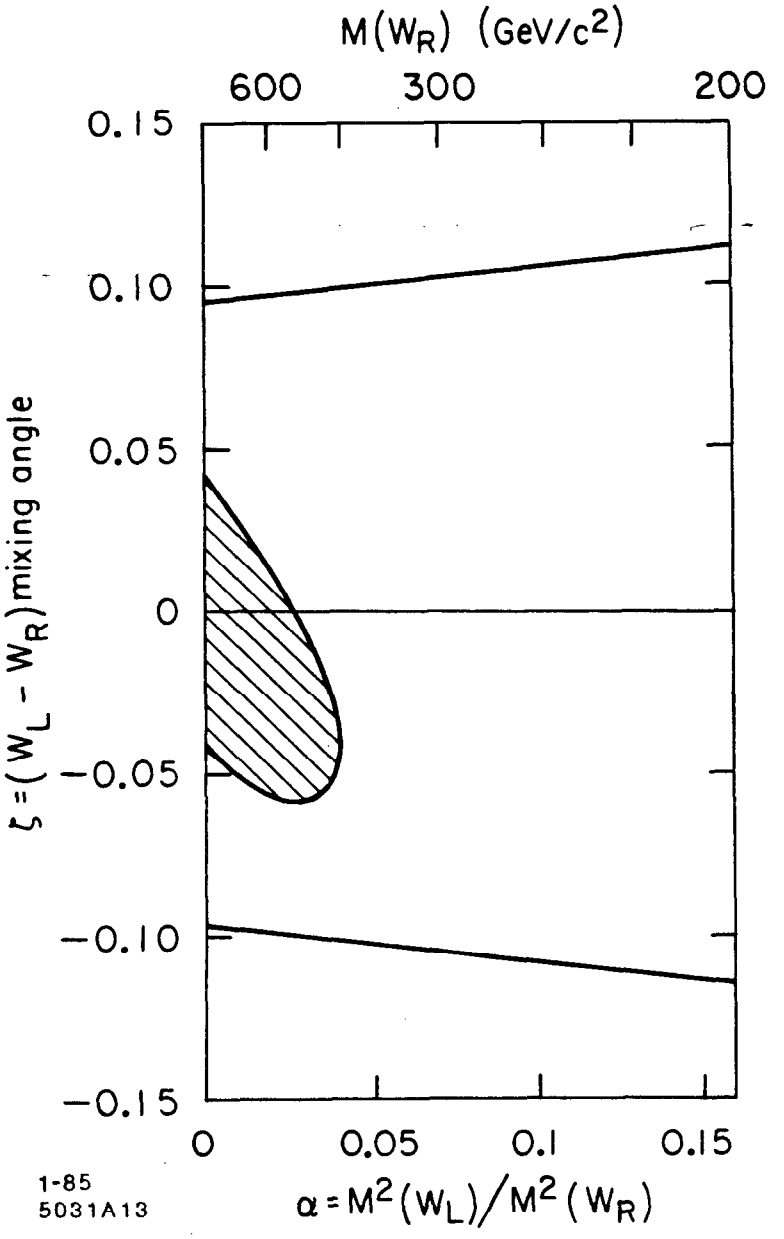
M(W_R) (GeV/c^2)
600
300
200
0.15
0.10
0.05
0
−0.05
−0.10
−0.15
ζ = (W_L − W_R) mixing angle
0
0.05
0.1
0.15
α = M^2(W_L)/M^2(W_R)
1-85
5031A13

Fig. 21

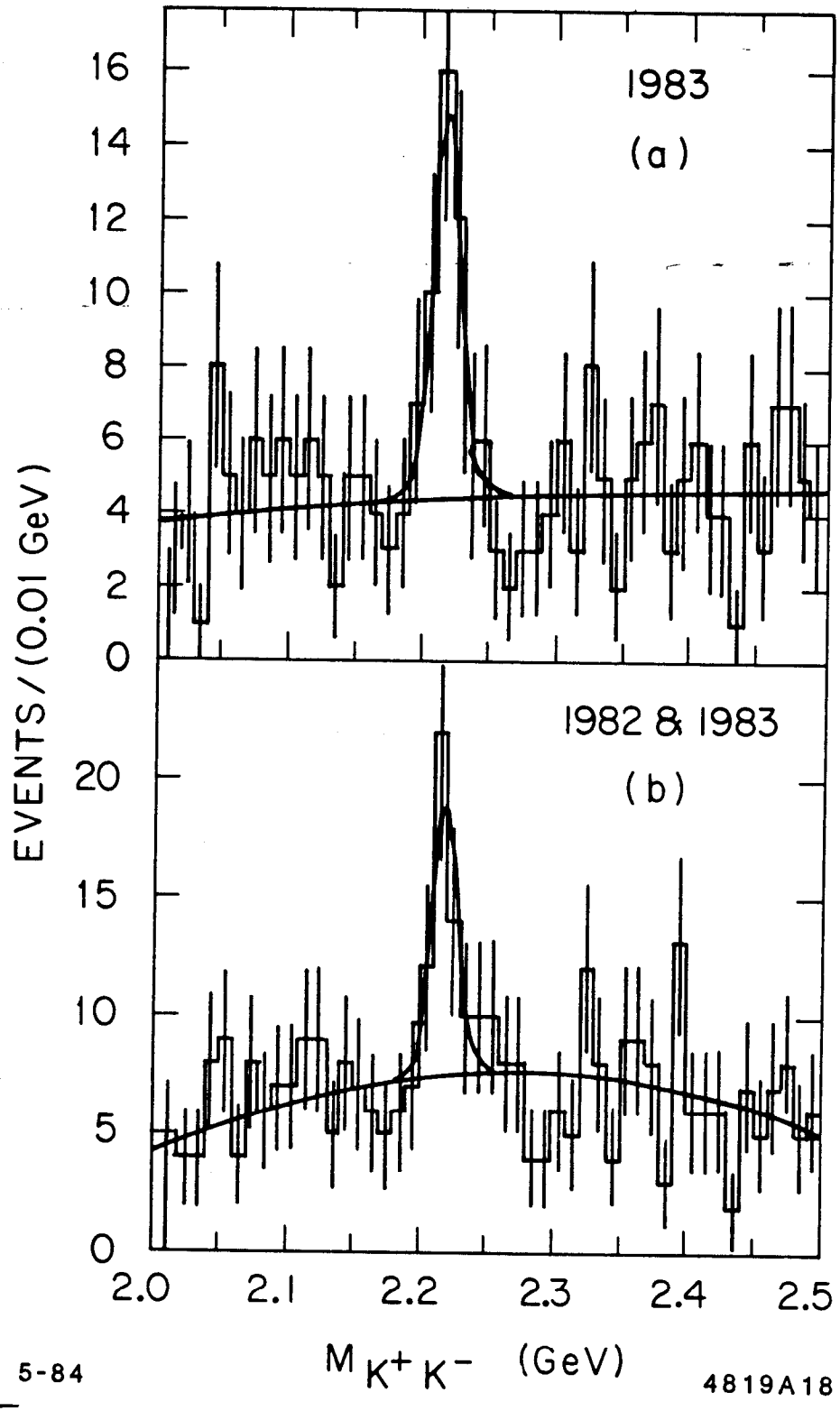
1983
(a)
1982 & 1983
(b)
EVENTS / (0.01 GeV)
0
2
4
6
8
10
12
14
16
0
5
10
15
20
2.0
2.1
2.2
2.3
2.4
2.5
$M_{K^+K^-}$ (GeV)
5-84
4819A18

Fig. 22

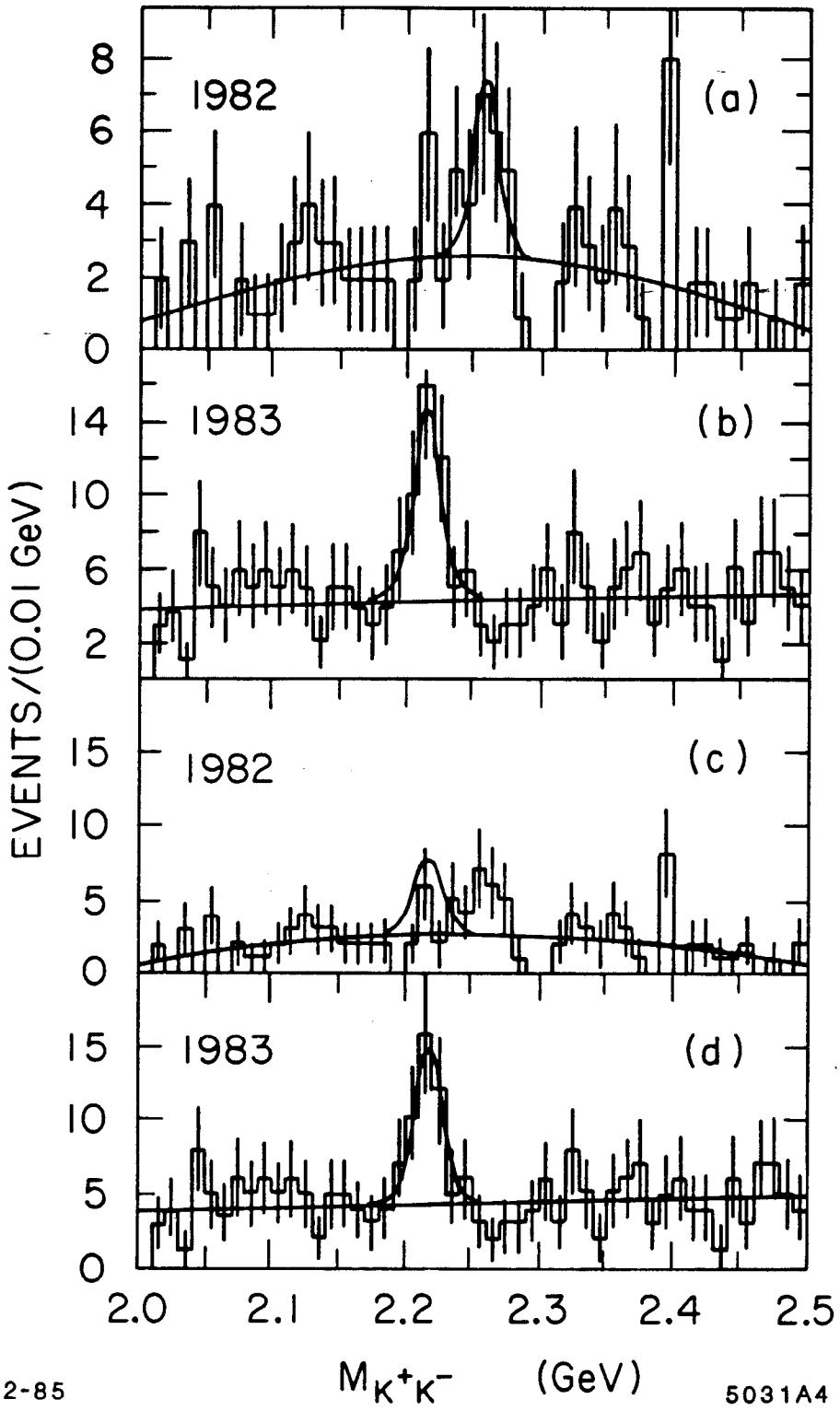

Fig. 23

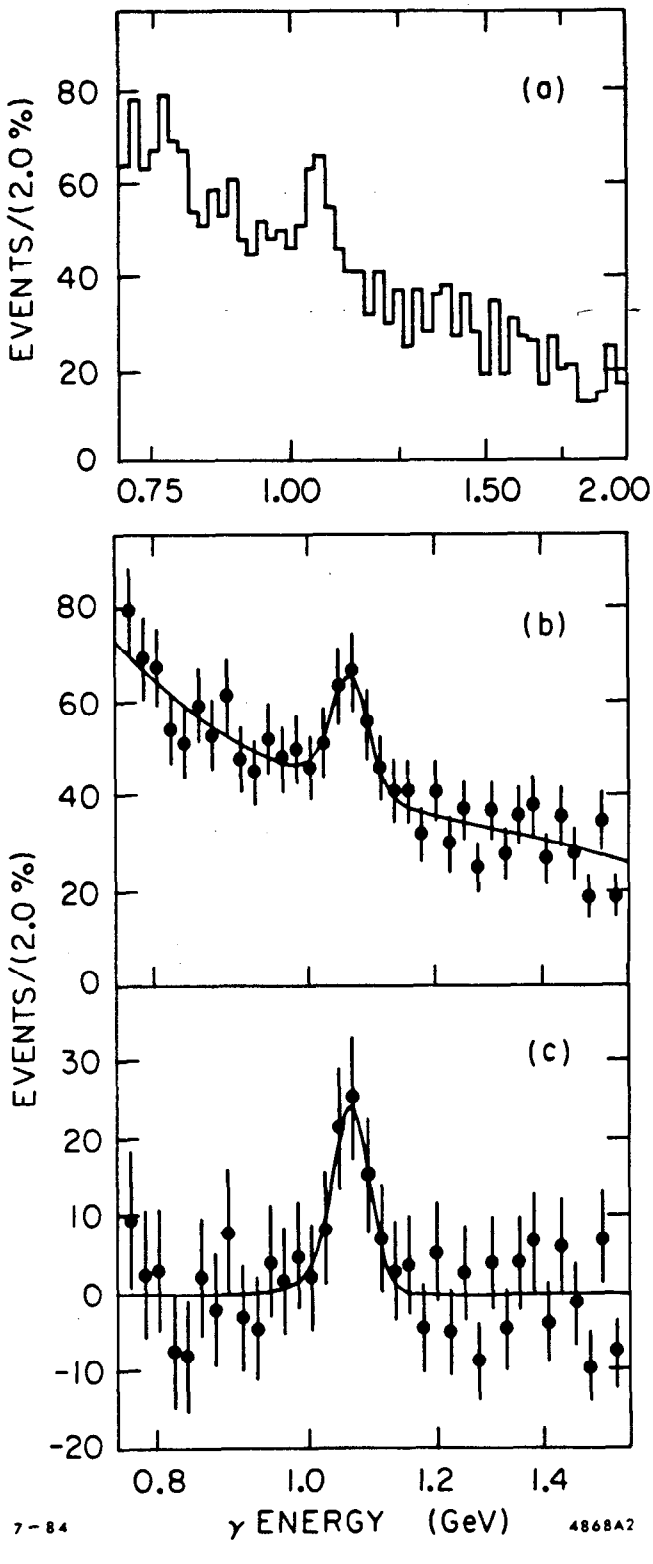
(a)
(b)
(c)
EVENTS/(2.0 %)
EVENTS/(2.0 %)
80
60
40
20
0
30
10
-10
-20
0.75
1.00
1.50
2.00
0.8
1.0
1.2
1.4
γ ENERGY (GeV)
7-84
4868A2

Fig. 24

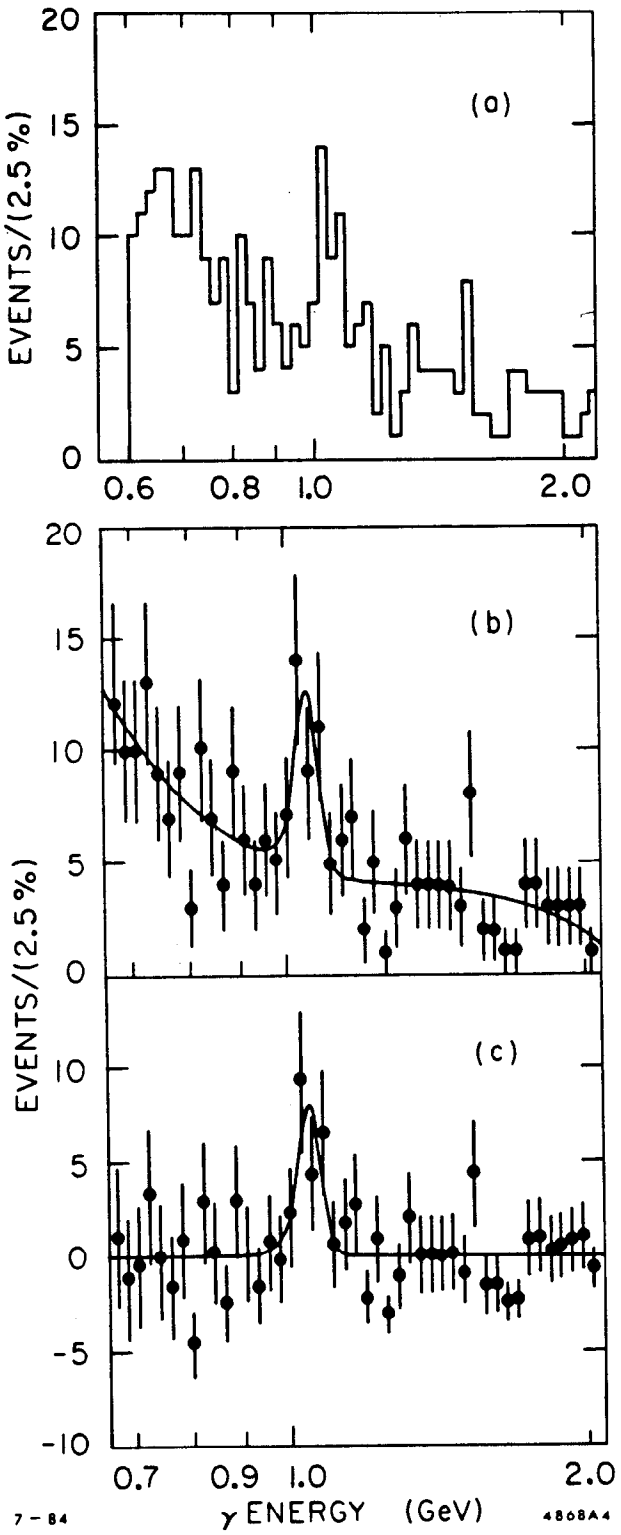
(a)
(b)
(c)
EVENTS/(2.5 %)
EVENTS/(2.5 %)
γ ENERGY (GeV)
0.6
0.8
1.0
2.0
0.7
0.9
1.0
2.0
7-84
4808A4

Fig. 25

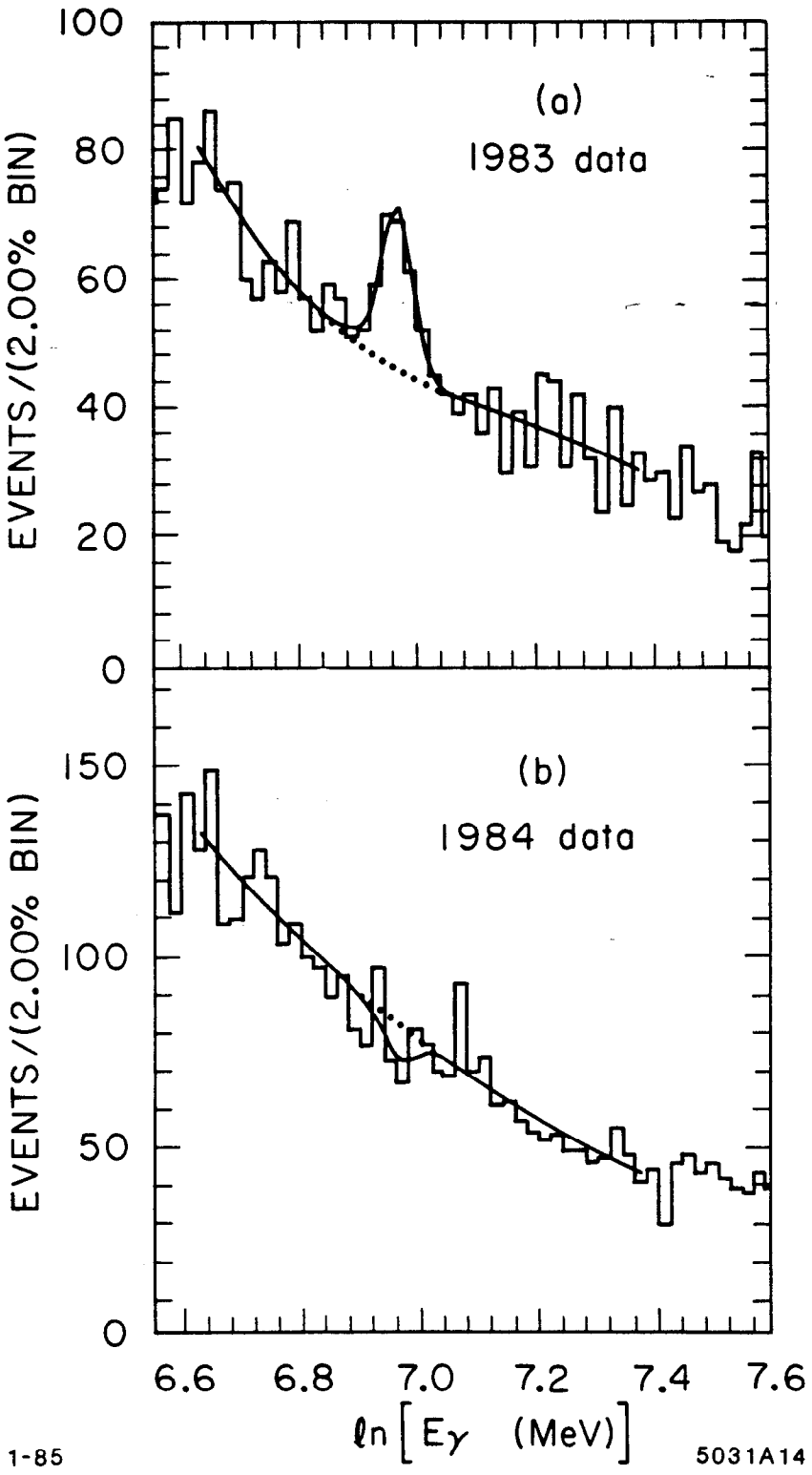
100
80
60
40
20
0
EVENTS/(2.00% BIN)
(a)
1983 data
150
100
50
0
EVENTS/(2.00% BIN)
(b)
1984 data
6.6
6.8
7.0
7.2
7.4
7.6
ln [Eγ (MeV)]
1-85
5031A14

Fig. 26

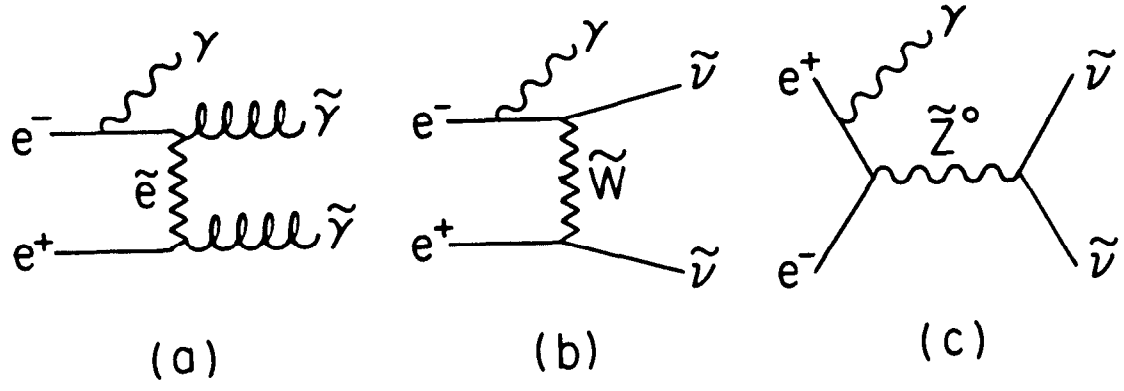

2-85

5031A15

Fig. 27

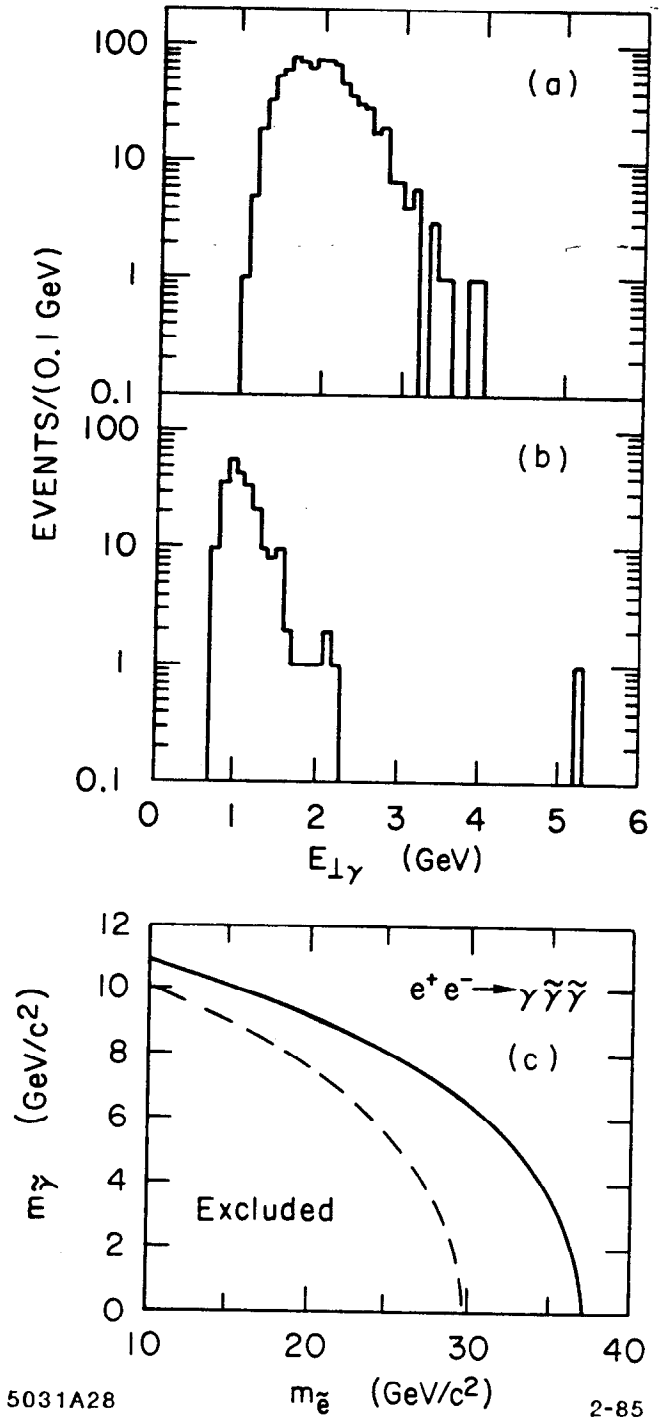
100
10
1
0.1
(a)
EVENTS/(0.1 GeV)
100
10
1
0.1
(b)
0 1 2 3 4 5 6
$E_{\perp\gamma}$ (GeV)
12
10
8
6
4
2
0
$e^+e^- \rightarrow \gamma\tilde{\gamma}\tilde{\gamma}$
(c)
Excluded
$m_{\tilde{\gamma}}$ (GeV/c²)
10 20 30 40
$m_{\tilde{e}}$ (GeV/c²)
5031A28
2-85

Fig. 28